IMMUNOLOGY

Armored human CAR T_{reg} cells with PD1 promoter-driven IL-10 have enhanced suppressive function

Dominic A. Boardman[1,2]†, Sonya Mangat[1,2,3]†, Jana K. Gillies[1,2], Lorna Leon[1,2], Vivian C. W. Fung[1,2], Manjurul Haque[1,2], Majid Mojibian[1,2], Torin Halvorson[1,2], Qing Huang[1,2], Karoliina Tuomela[1,2], Christine M. Wardell[1,2], Andrew Brown[1,2], Avery J. Lam[4], Megan K. Levings[1,2,5]*

Regulatory T cell (T_{reg} cell) therapy has been transformed through the use of chimeric antigen receptors (CARs). We previously found that human T_{reg} cells minimally produce IL-10 and have a limited capacity to control innate immunity compared to type 1 regulatory T cells (T_r1 cells). To create "hybrid" CAR T_{reg} cells with T_r1 cell-like properties, we examined whether the *PDCD1* locus could be exploited to endow T_{reg} cells with CAR-regulated IL-10 expression. CRISPR-mediated PD1 deletion increased CAR T_{reg} cell activation, and knock-in of *IL10* under control of the PD1 promoter resulted in CAR-induced IL-10 secretion. *IL10* knock-in improved CAR T_{reg} cell function, as determined by increased suppression of dendritic cells and alloantigen- and islet autoantigen–specific T cells. In vivo, *IL10* knock-in CAR T_{reg} cells were stable, safe, and suppressed dendritic cells and xenogeneic graft-versus-host disease. CRISPR-mediated engineering to simultaneously remove an inhibitory signal and enhance a suppressive mechanism is a previously unexplored approach to improve CAR T_{reg} cell potency.

INTRODUCTION

Adoptive transfer of regulatory T cells (T_{reg} cells) is a promising therapeutic strategy for treating transplant rejection, as well as a variety of autoimmune diseases and inflammatory disorders (*1*). Clinical trials have shown that polyclonal T_{reg} cell therapy is feasible and well tolerated (*2*, *3*), but it is generally thought that efficacy is limited without enrichment for antigen-specific cells. Numerous groups have thus explored the potential to use chimeric antigen receptors (CARs) to confer disease-relevant antigen specificity to T_{reg} cells. CARs are synthetic fusion proteins that use domains from various receptors to redirect the specificity of T cells toward desired antigens of interest (*4*). We and others used CAR technology to redirect T_{reg} cell specificity to human leukocyte antigen (HLA)-A2, finding that CAR expression significantly improves human T_{reg} cell potency in humanized mouse models of transplantation (*5*–*8*). However, in immunocompetent mouse transplant models, HLA-A2–specific CAR (A2-CAR) T_{reg} cells do not induce indefinite graft survival (*9*, *10*), suggesting that additional engineering may be required to fully unlock the protective capacity of these cells.

Programmed cell death protein 1 (PD1) is an immune checkpoint molecule that is up-regulated in T cells and T_{reg} cells following activation (*11*). In cancer research, multiple studies explored PD1 deletion as a strategy to limit T cell exhaustion (*12*–*15*), finding that PD1-deficient T cells may have extended persistence compared to PD1-sufficient counterparts. In T_{reg} cells, evidence suggests that PD1 has a similar negative role. Upon ligand (PD-L1 or PD-L2) engagement, PD1 triggers intracellular signaling cascades that inhibit T_{reg} cell activation and function (*8*, *16*, *17*). High PD1 expression in human T_{reg} cells is correlated with reduced suppressive function in cancer (*16*) and multiple sclerosis (*18*), and in vitro, antibody-mediated blockade of PD1:PD-L1 interactions improves T_{reg} cell function (*19*–*21*). Similarly, in mice, PD1:PD-L1 blockade promotes T_{reg} cell activity, enhancing their ability to alleviate lupus-like disease (*22*). T_{reg} cell–specific PD1 deletion also ameliorates experimental autoimmune encephalomyelitis (EAE) and protects nonobese diabetic (NOD) mice from type 1 diabetes (*23*). Together, these observations suggest that removal of PD1 in therapeutic CAR T_{reg} cells may benefit their function.

T_{reg} cells suppress immune responses via multiple mechanisms, one of which is production of anti-inflammatory cytokines such as transforming growth factor (TGF)–β and interleukin-10 (IL-10). However, the amounts of IL-10 secreted by human T_{reg} cells isolated from blood are relatively low (*24*–*26*), particularly in comparison to type 1 regulatory T cells (T_r1 cells) that are defined by high IL-10 secretion (*27*). IL-10 primarily acts on myeloid cells to suppress pro-inflammatory cytokine production and limit antigen-presenting cell (APC) function, in turn suppressing adaptive immune cell activation (*28*). Due to low IL-10 production from mouse and human T_{reg} cells, they are less able to suppress innate immune responses compared to T_r1 cells (*25*, *26*), possibly resulting in suboptimal linked and/or bystander suppression which is thought to be critical for tolerance induction (*29*, *30*). Endowing T_{reg} cells with the ability to secrete high levels of IL-10 in an activation-dependent manner may overcome this limitation and enhance their therapeutic efficacy.

In this study, we explored whether the activation potential and immunosuppressive function of CAR T_{reg} cells could be enhanced by ablating PD1 using CRISPR. In addition, we examined whether the endogenous *PDCD1* promoter could be exploited to control expression of an exogenous IL-10 transgene, thereby further improving the immunoregulatory function of CAR T_{reg} cells.

RESULTS

Manufacturing armored CAR T_{reg} cells

To generate PD1-deficient CAR T_{reg} cells, two gene editing procedures were performed: (i) lentiviral transduction to deliver an HLA-A2–specific CAR (A2-CAR; Fig. 1A) and (ii) CRISPR editing

[1]Department of Surgery, The University of British Columbia, Vancouver, BC, Canada. [2]BC Children's Hospital Research Institute, Vancouver, BC, Canada. [3]Department of Microbiology and Immunology, The University of British Columbia, Vancouver, BC, Canada. [4]Department of Pathology, Stanford University, Stanford, CA, USA. [5]School of Biomedical Engineering, The University of British Columbia, Vancouver, BC, Canada.
*Corresponding author. Email: mlevings@bcchr.ca
†These authors contributed equally to this work.

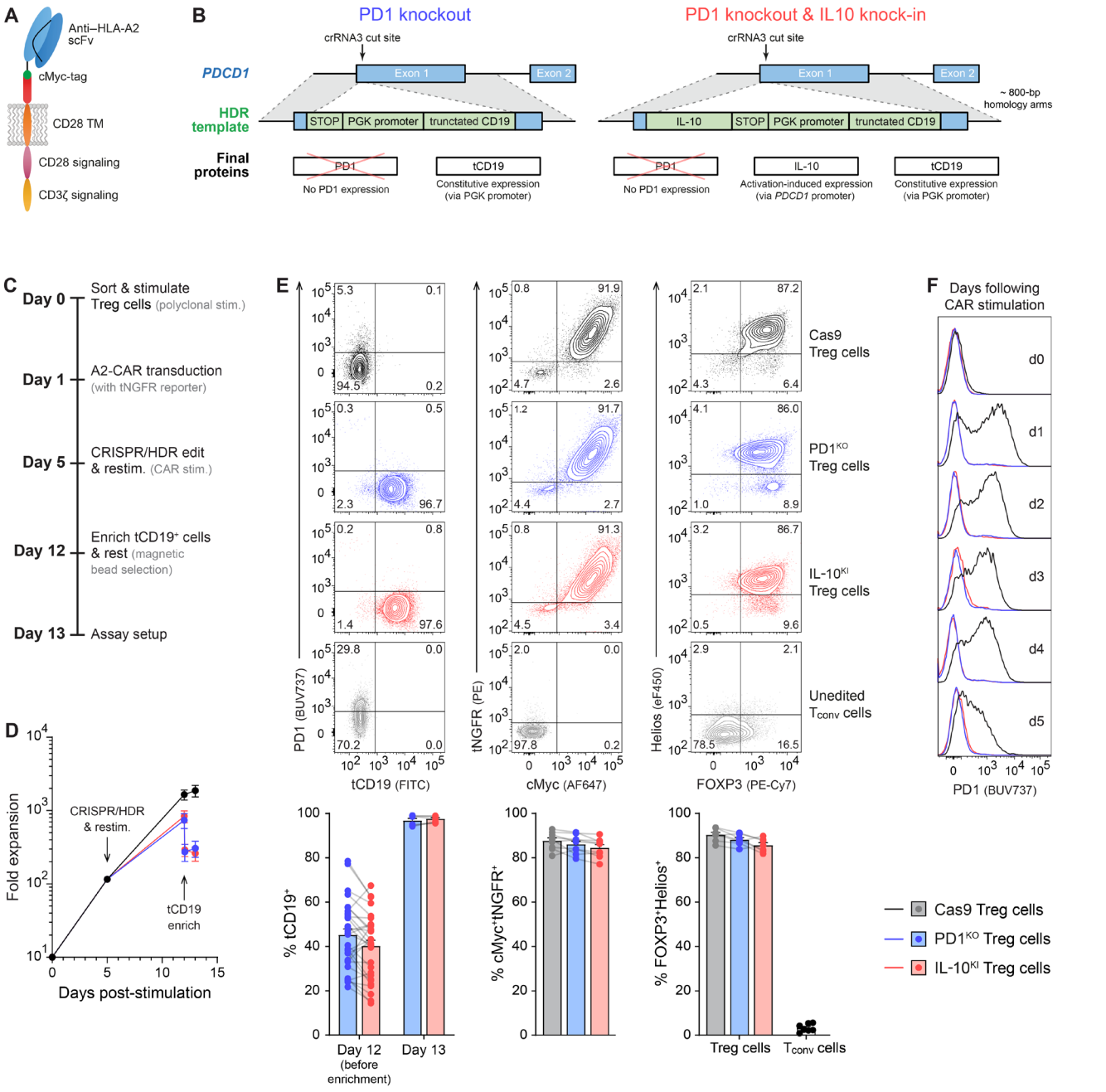

Fig. 1. Manufacturing PD1^{KO} and IL-10^{KI} A2-CAR T$_{reg}$ cells. (**A**) Schematic diagram of the second-generation HLA-A2–specific CAR (A2-CAR) used throughout the study. (**B**) Schematic diagram of the *PDCD1* locus and homology-directed repair templates (HDRTs). (**C**) Timeline for manufacturing gene-edited T$_{reg}$ cells. (**D**) T$_{reg}$ cell expansion during manufacture, with time points of CRISPR editing and selection of tCD19$^+$ cells indicated. (**E**) Representative (top) and average (bottom) data from phenotypic characterization of the different types of A2-CAR T$_{reg}$ cells as well as unedited T$_{conv}$ cells, gated on live CD4$^+$ cells. (**F**) PD1 expression in A2-CAR T$_{reg}$ cells following stimulation with HLA-A2$^+$PD-L1$^-$ K562 cells. Gated on live CD4$^+$cMyc$^+$tNGFR$^+$ and tCD19$^+$ cells, where appropriate. Averaged data are means ± SEM with lines connecting data points from individual subjects (n = 3 to 33). FITC, fluorescein isothiocyanate. AF647, Alexa Fluor 647; PE-Cy7, Phycoerythrin-Cyanine 7; BUV737, Brilliant UltraViolet 737.

to ablate PD1 (Fig. 1B). Naïve CD4$^+$CD25^{hi}CD127^{lo}CD45RA$^+$CD45RO$^-$ cells were sorted from the peripheral blood of healthy subjects and stimulated with artificial APCs (aAPCs) loaded with anti-CD3 (Fig. 1C). After 24 hours, T$_{reg}$ cells were transduced with a lentiviral vector encoding a second-generation A2-CAR under control of the elongation factor (EF)1α promoter, and a truncated nerve growth factor receptor (tNGFR) reporter driven by a minimal cytomegalovirus (CMV) promoter (*5*, *8*).

On day 5, T$_{reg}$ cells were electroporated with Cas9 protein alone (Cas9 T$_{reg}$ cells) or ribonuclear protein (RNP) complexes containing a *PDCD1*-specific guide RNA (gRNA; crRNA3) that efficiently ablated PD1 (fig. S1). For the latter conditions, a homology-directed

repair template (HDRT) was delivered by adeno-associated virus serotype 6 (AAV6) transduction such that PD1-deficient T_{reg} cells (hereafter referred to as $PD1^{KO}$ T_{reg} cells) could be identified by constitutive expression of a truncated CD19 (tCD19) reporter driven by a phosphoglycerate kinase (PGK) promoter (Fig. 1B, left). Alternatively, an HDRT containing a promoterless *IL10* open reading frame (ORF), in addition to the PGK-driven tCD19 reporter, was delivered into the *PDCD1* locus such that the endogenous cellular machinery that typically controls *PDCD1* would instead control expression of *IL10* (hereafter referred to as $IL\text{-}10^{KI}$ T_{reg} cells; Fig. 1B, right). In the HDRT design illustrated in Fig. 1B, the cut site of crRNA3 resulted in addition of five amino acids (MQIPQ) at the N terminus, which did not affect IL-10 secretion or immunosuppressive function (fig. S2).

Following electroporation, T_{reg} cells were restimulated with $HLA\text{-}A2^+$ aAPCs to preferentially expand $A2\text{-}CAR^+$ cells for an additional 7 days. On day 12 of culture, successfully edited $tCD19^+$ cells were enriched using magnetic bead selection and rested overnight with a low dose of IL-2 in preparation for assays that were performed on day 13 (Fig. 1C).

During expansion, Cas9 T_{reg} cells had a minor growth advantage compared to the homology directed repair (HDR)-edited T_{reg} cells (Fig. 1D), but no phenotypic differences were observed between the three types of T_{reg} cells at the time of assay setup (Fig. 1E). $PD1^{KO}$ and $IL\text{-}10^{KI}$ T_{reg} cells were edited with a HDR efficiency of ~40% and enriched to a purity of >95% (Fig. 1E, left). As determined by staining for the cellular myelocytoma (cMyc) tag present in the extracellular domain of the CAR construct (Fig. 1E, middle), >85% of the T_{reg} cells expressed the A2-CAR on their cell surface, and all T_{reg} cells maintained their expected constitutive expression of FOXP3 and Helios (Fig. 1E, right).

To test efficacy of PD1 protein deletion, CAR-induced expression of PD1 was measured by flow cytometry. As expected, control Cas9 T_{reg} cells up-regulated PD1, whereas no PD1 expression was observed for $PD1^{KO}$ or $IL\text{-}10^{KI}$ CAR T_{reg} cells (Fig. 1F). Upon CAR stimulation with $HLA\text{-}A2^+PD\text{-}L1^+$ aAPC, $PD1^{KO}$ T_{reg} cells also expressed significantly higher levels of activation markers, compared to Cas9 T_{reg} cells, confirming the beneficial effects of removing this negative regulator of T cell activation (fig. S3) (*31*). Overall, these results demonstrate that human T_{reg} cells can be lentivirally transduced and CRISPR-edited without influencing their characteristic expression of FOXP3 and Helios.

CAR-stimulation induces IL-10 secretion by $IL\text{-}10^{KI}$ T_{reg} cells

To assess whether $IL\text{-}10^{KI}$ T_{reg} cells secreted IL-10 in response to CAR stimulation, T_{reg} cells were cocultured with $HLA\text{-}A2^+PD\text{-}L1^-$ aAPCs for 72 hours, and supernatants were analyzed for cytokine secretion. We found that CAR-stimulated $IL\text{-}10^{KI}$ T_{reg} cells secreted ~20-fold more IL-10 than unstimulated $IL\text{-}10^{KI}$ T_{reg} cells (Fig. 2A), confirming activation-induced IL-10 expression. Furthermore, $IL\text{-}10^{KI}$ T_{reg} cells secreted significantly more IL-10 than Cas9, $PD1^{KO}$ T_{reg} cells, or T_r1 cells (*27*) upon CAR stimulation. All T_{reg} cell groups expressed low levels of pro-inflammatory cytokines, particularly when compared to T_r1 cells (Fig. 2B).

Next, we compared the relative secretion of 11 T cell–related cytokines and found that the primary cytokine secreted by $IL\text{-}10^{KI}$ T_{reg} cells was IL-10, making up 62.7% of the total quantity of cytokines analyzed (Fig. 2C). In contrast, while T_r1 cells also secreted high quantities of IL-10 (Fig. 2A), they produced high levels of pro-inflammatory cytokines [e.g. interferon-γ (IFN-γ), IL-17A, and tumor necrosis factor–α (TNFα); Fig. 2B], making the relative proportion of IL-10 secreted in comparison to pro-inflammatory cytokines low (only 1.9% of total cytokine quantities analyzed; Fig. 2C).

CAR T_{reg} cells that constitutively overexpress IL-10 via lentiviral (LV–IL-10) transduction have been previously described (*32*). To compare the IL-10 secretion by $IL\text{-}10^{KI}$ T_{reg} cells versus LV–IL-10 CAR T_{reg} cells, we created an LV construct encoding *IL10* under control of the EF1α promoter. LV–IL-10 T_{reg} cells were generated by transducing T_{reg} cells with two vectors: one enabling CAR expression and the other enabling constitutive IL-10 expression. In the absence of CAR stimulation, LV–IL-10 T_{reg} cells secreted >80-fold more IL-10 than $IL\text{-}10^{KI}$ T_{reg} cells (fig. S4A), demonstrating the improved regulation of IL-10 secretion using the CRISPR-mediated knock-in strategy. In response to CAR stimulation, LV–IL-10 T_{reg} cells secreted >200-fold more IL-10 than $IL\text{-}10^{KI}$ T_{reg} cells, likely due to the multiple genomic integrations achieved by the lentiviral transduction process. However, this additional IL-10 secretion did not improve the ability of the LV–IL-10 T_{reg} cells to suppress HLA-A2–expressing dendritic cells (DCs) over $IL\text{-}10^{KI}$ T_{reg} cells (fig. S4B). In the presence of HLA-A2, $IL\text{-}10^{KI}$ and LV–IL-10 T_{reg} cells were equally suppressive, but, in the absence of HLA-A2, $IL\text{-}10^{KI}$ T_{reg} cells performed similarly to untransduced T_{reg} cells, emphasizing that, unlike LV–IL-10 T_{reg} cells, $IL\text{-}10^{KI}$ T_{reg} cells function in an antigen-dependent manner.

In addition to increasing the total amount of IL-10 secreted, control of *IL10* by the *PDCD1* promoter also had the potential to alter the kinetics of IL-10 secretion. To assess this, we measured cytokine secretion in 24-hour windows poststimulation (Fig. 2D and fig. S5) by stimulating with $HLA\text{-}A2^+$ $PD\text{-}L1^-$ aAPCs cells and collecting cell culture supernatants every 24 hours. Cas9/$PD1^{KO}$ T_{reg} cells and T_r1 cells all secreted the most IL-10 within the first 24 hours, and this steadily diminished over time. In contrast, $IL\text{-}10^{KI}$ T_{reg} cells secreted IL-10 with a unique kinetic profile that peaked ~72 hours poststimulation. The amount of IFN-γ (Fig. 2D, right), as well as other pro-inflammatory cytokines (fig. S5), secreted by $IL\text{-}10^{KI}$ T_{reg} cells remained low in comparison to T_r1 cells.

To further investigate the kinetics of *IL10* expression, quantitative polymerase chain reaction (qPCR) was used to measure amounts of endogenous versus exogenous mRNA (Fig. 2E). The kinetics of total *IL10* mRNA synthesis were comparable to IL-10 protein secretion (Fig. 2D, left), with $IL\text{-}10^{KI}$ T_{reg} cells expressing more *IL10* than Cas9 T_{reg} cells, and exhibiting peak expression 3 to 4 days poststimulation. $IL\text{-}10^{KI}$ T_{reg} cells also had higher expression of endogenous *IL10*, suggesting a positive feedback loop, as previously described for T_r1 cells (*33*, *34*) and T_{reg} cells (*35*). Consistent with the protein data, even without CAR stimulation, there was some endogenous and exogenous *IL10* mRNA expression in $IL\text{-}10^{KI}$ T_{reg} cells; however, in all assays, amounts were higher in CAR-stimulated cells. Overall, these results demonstrate that upon CAR stimulation, $IL\text{-}10^{KI}$ T_{reg} cells secrete significantly greater quantities of IL-10 for a longer duration than control T_{reg} cells and T_r1 cells.

$IL\text{-}10^{KI}$ T_{reg} cells retain their core transcriptome

To more comprehensively test how CRISPR editing, *PDCD1* knockout and *IL10* knock-in affected T_{reg} cells, we performed RNA sequencing (RNA-seq). T_{reg} cells, T_r1 cells, and $CD4^+$ conventional T cells (T_{conv} cells) were stimulated via their CAR for 16 hours, after which total RNA was extracted and analyzed. A principal component

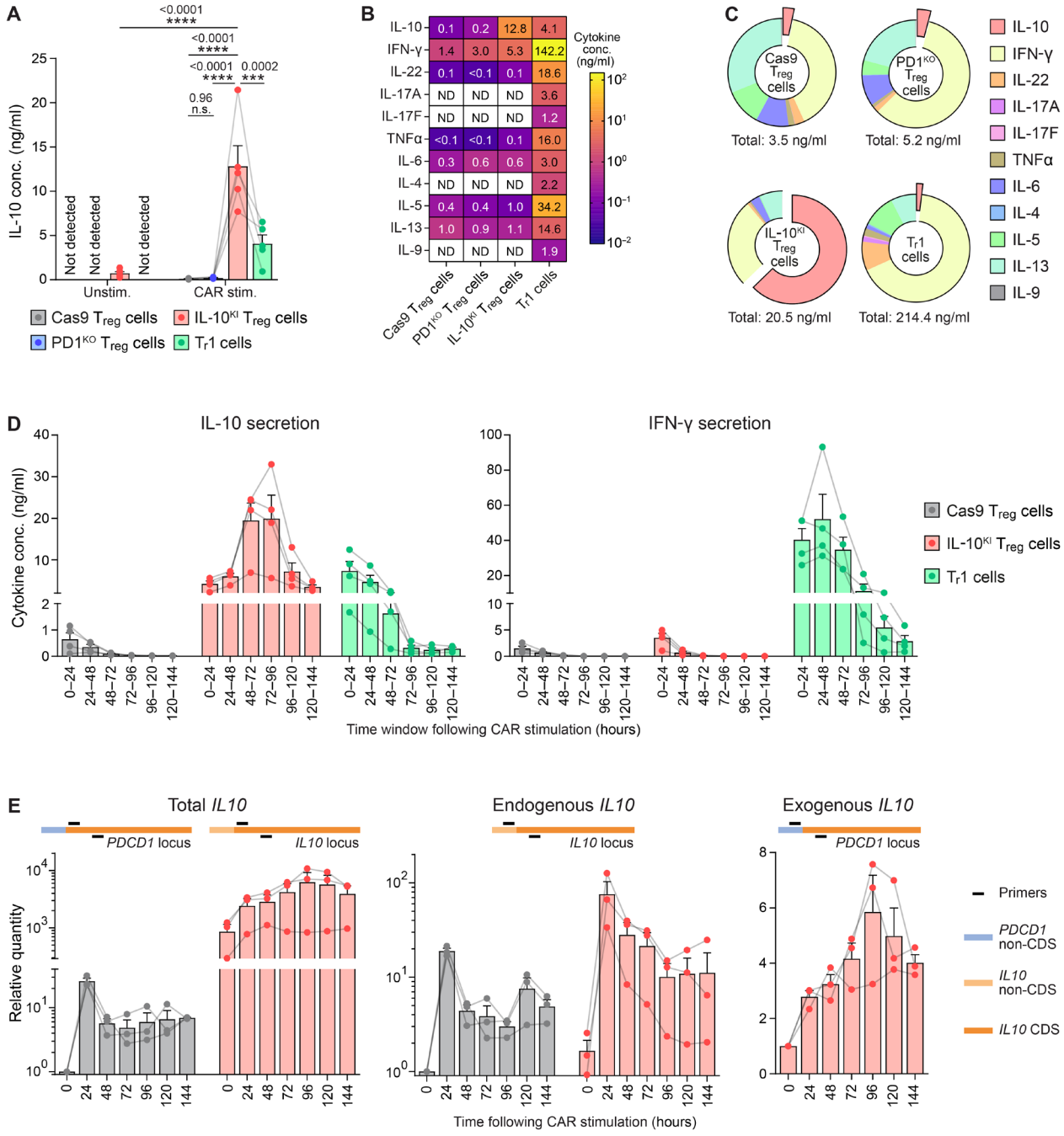

Fig. 2. IL-10^{KI} T$_{reg}$ cells secrete IL-10 following CAR stimulation. (**A** to **C**) Different types of A2-CAR T$_{reg}$ cells and A2-CAR T$_r$1 cells were stimulated with blank (Unstim.) or HLA-A2$^+$PD-L1$^-$ (CAR-stim.) K562 cells. After 72 hours, amounts of (A) IL-10 and (B) other cytokines were measured. In (C), cytokine data are expressed as doughnut plots to show the relative amount of IL-10 as a proportion of the 11 cytokines analyzed. The summed ng/ml of all 11 cytokines measured is provided below each doughnut plot. (**D**) A2-CAR T$_{reg}$ cells and T$_r$1 cells were stimulated with HLA-A2$^+$PD-L1$^-$ K562 cells. Every 24 hours, cell supernatants were collected, the cells were washed twice with PBS, and replated in fresh medium with IL-2. (**E**) Quantitative polymerase chain reaction (qPCR) analysis of T$_{reg}$ cell *IL10* expression following coculture with HLA-A2$^+$PD-L1$^-$ K562 cells. qPCRs were performed using primers that amplified mRNA corresponding to total *IL10* (left), endogenous *IL10* (middle), and exogenous *IL10* (right). Schematic diagrams showing primer recognition sites are provided. CDS, coding sequence. Averaged data are means ± SEM with connecting data points from individual subjects (n = 3 to 5). Statistical significance was determined using mixed-effects analysis tests with P values shown. ND, not detected.

analysis confirmed that IL-10^{KI} T_{reg} cells cluster with Cas9 and PD1^{KO} T_{reg} cells, while T_r1 cells and T_{conv} cells clustered separately (Fig. 3A). There were only 28 differentially expressed genes (DEGs) between Cas9 and IL-10^{KI} T_{reg} cells (Fig. 3, B and C), with *IL10* notably among these genes, showing that IL-10^{KI} T_{reg} cells retained their core gene signature. Conversely, IL-10^{KI} T_{reg} cells and T_r1 cells differentially expressed 1273 genes, with 916 of these genes also differentially expressed between Cas9 T_{reg} cells and T_r1 cells (Fig. 3, B and C).

Taking advantage of the N-terminal addition of 15 bases of the knocked-in IL-10 (fig. S2A), we analyzed the RNA-seq data to further compare amounts of endogenous versus exogenous *IL10*. Consistent with the qPCR data (Fig. 2E), IL-10^{KI} T_{reg} cells had significantly higher expression of endogenous, exogenous, and total *IL10* compared to Cas9/PD1^{KO} T_{reg} cells and T_r1 cells (Fig. 3D).

Further analysis of secreted factors (Fig. 3E) and T cell/T_{reg} cell–associated genes (Fig. 3F) (*26*, *36*) revealed that Cas9, PD1^{KO}, and IL-10^{KI} T_{reg} cells had similar transcriptome profiles. Among the few significant differences, IL-10^{KI} T_{reg} cells expressed higher *IL2RA* and lower *IL7R* mRNA (Fig. 3F). In contrast to T_{reg} cells, T_r1 cells expressed high levels of pro-inflammatory cytokines including IL-2, IL-5, IL-13, and IL-17F (Fig. 3, C, bottom, and E), consistent with data in Fig. 2 and fig. S5. These distinct differences in transcriptomes between T_{reg} cells and T_r1 cells were accentuated by a comparison of the top 50 DEGs and are consistent with our previous findings (*26*). Overall, IL-10^{KI} T_{reg} cells retain their characteristic gene signature and remain distinct from T_r1 cells.

IL-10^{KI} T_{reg} cells skew the differentiation of DCs toward a tolerogenic phenotype

IL-10 acts on innate immune cells, including DCs, to suppress differentiation to mature cells and antigen presentation (*28*, *37*–*39*). To assess the effect of IL-10^{KI} T_{reg} cells on DC differentiation, HLA-A2$^+$CD14$^+$ monocytes were cocultured with T_{reg} cells in the presence of granulocyte-macrophage colony-stimulating factor (GM-CSF) and IL-4, and, after 7 days, the monocyte-derived DC (moDC) phenotype was measured by flow cytometry (Fig. 4A).

IL-10^{KI} T_{reg} cells significantly promoted the expression of CD141, CD163, HLA-G, and CD14 (Fig. 4, B to D), resulting in a phenotype resembling that of DC10 cells, immunoregulatory DCs that promote T_r1 cell differentiation and infectious tolerance (*33*, *34*). In contrast, untransduced, Cas9, and PD1^{KO} T_{reg} cells did not significantly affect DC differentiation. IL-10^{KI} T_{reg} cell–exposed moDCs down-regulated CD86 but up-regulated CD80, consistent with the divergent expression of CD80 and CD86 on DC10 cells (*33*, *34*).

To test how IL-10^{KI} T_{reg} cells affected DC cytokine production, following T_{reg} cell/DC coculture, CD11c$^+$CD4$^-$ DCs were isolated by cell sorting and stimulated with lipopolysaccharide (LPS) and IFN-γ, and, after 24 hours, supernatants were analyzed for cytokine secretion. IL-10^{KI} T_{reg} cell–treated moDCs secreted significantly less TNFα (PD1^{KO} versus IL-10^{KI}, $P = 0.0009$), IL-12p40 (Cas9 versus IL-10^{KI}, $P < 0.0001$), CCL17 (Cas9 versus IL-10^{KI}, $P = 0.0002$), and CXCL10 (Cas9 versus IL-10^{KI}, $P = 0.0012$, mixed-effects analysis) (Fig. 4E). Overall, these data show that IL-10^{KI} T_{reg} cells promote the differentiation of moDCs with a tolerogenic phenotype.

IL-10^{KI} T_{reg} cells suppress the antigen presenting capacity of mDCs

We next tested how IL-10^{KI} T_{reg} cells influenced the antigen presenting capacity of differentiated, mature DCs (mDCs). We first tested the effects of recombinant IL-10 (rIL-10), finding only subtle effects on suppression of CD80 and CD86. However, effects of rIL-10 were enhanced when combined with CAR T_{reg} cells, demonstrating strong, synergistic suppression by IL-10 and CAR T_{reg} cells (Fig. 5A).

To measure the effects of T_{reg} cells on HLA-A2$^+$ mDCs, cells were cocultured for 72 hours, after which the DC phenotype was measured by flow cytometry (Fig. 5B). As expected (*8*), CAR expression significantly improved T_{reg} cell–mediated suppression of DC co-stimulatory molecules, with the IL-10^{KI} T_{reg} cells showing a superior effect (Fig. 5, C and D). No effects on HLA-DR expression were observed (fig. S6A). PD1 deletion did not enhance suppression of co-stimulatory molecules, but PD1^{KO} T_{reg} cells did significantly induce PD-L1 expression on mDC, an effect further accentuated by IL-10^{KI} T_{reg} cells, as has previously been demonstrated in studies assessing T_{reg} cells in a cancer setting (*35*). None of the T_{reg} cell types affected mDC viability (fig. S6B). Overall, these results demonstrate that IL-10^{KI} T_{reg} cells have an enhanced capacity to suppress co-stimulatory molecule expression on pro-inflammatory mDCs.

IL-10^{KI} T_{reg} cells have enhanced suppression of allo- and autoreactive T cells

T_{reg} cells dampen deleterious immune responses by suppressing a range of cells including innate and adaptive immune cells. To investigate whether replacing *PDCD1* with *IL10* improved the ability of T_{reg} cells to inhibit T cell proliferation, a variety of suppression assays were performed. Initial assays were performed in a polyclonal manner whereby T_{reg} cells were cocultured with cell proliferation dye (CPD)–labeled responder peripheral blood mononuclear cells (PBMCs) in the presence of anti-CD3/CD28 beads, such that T_{reg} cells were stimulated via their T cell receptor (TCR) rather than their CAR (fig. S7A). In this setup, Cas9 and PD1^{KO} T_{reg} cells inhibited CD4$^+$ and CD8$^+$ responder T cell proliferation similarly, whereas IL-10^{KI} T_{reg} cells were more suppressive (fig. S7B). However, the improved suppressive effect of IL-10^{KI} T_{reg} cells on T cell proliferation in this system was subtle. To test whether this might be related to levels of IL-10 receptor (IL-10R) expression, we measured IL-10RA and IL-10RB expression on responder T cells following αCD3/CD28 stimulation, finding no expression without activation (fig. S8A). We also tested the effect of rIL-10 on αCD3/CD28-stimulated T cell proliferation and found no suppressive effect (fig. S8B). These data suggest that resting T cells are not susceptible to direct IL-10–mediated suppression. In contrast, analysis of CD19$^+$ responder B cells within the PBMCs revealed that IL-10^{KI} T_{reg} cells inhibited CD86 expression significantly more than Cas9 or PD1^{KO} T_{reg} cells (fig. S7C), consistent with the expected effect of IL-10 on APCs.

To address the limitation of the polyclonal suppression assay, we optimized two antigen- and APC-dependent suppression assays. In the first APC-dependent suppression assay system, T_{reg} cells were cocultured with HLA-A2$^+$ DCs and the subsequent capacity of these DCs to stimulate direct alloreactive responder T cells was assessed (Fig. 6A) (*40*). CAR-induced T_{reg} cell proliferation was confirmed to be equivalent for Cas9, PD1^{KO}, and IL-10^{KI} T_{reg} cells (fig. S9). CAR expression significantly enhanced the ability of T_{reg} cells to inhibit alloreactive T cell proliferation (Fig. 6, B and C). PD1 deletion in T_{reg} cells had a negligible effect, consistent with the finding that Cas9 and PD1^{KO} T_{reg} cells equally suppressed co-stimulatory molecule expression in mDCs (Fig. 5). In contrast, IL-10^{KI} T_{reg} cells suppressed

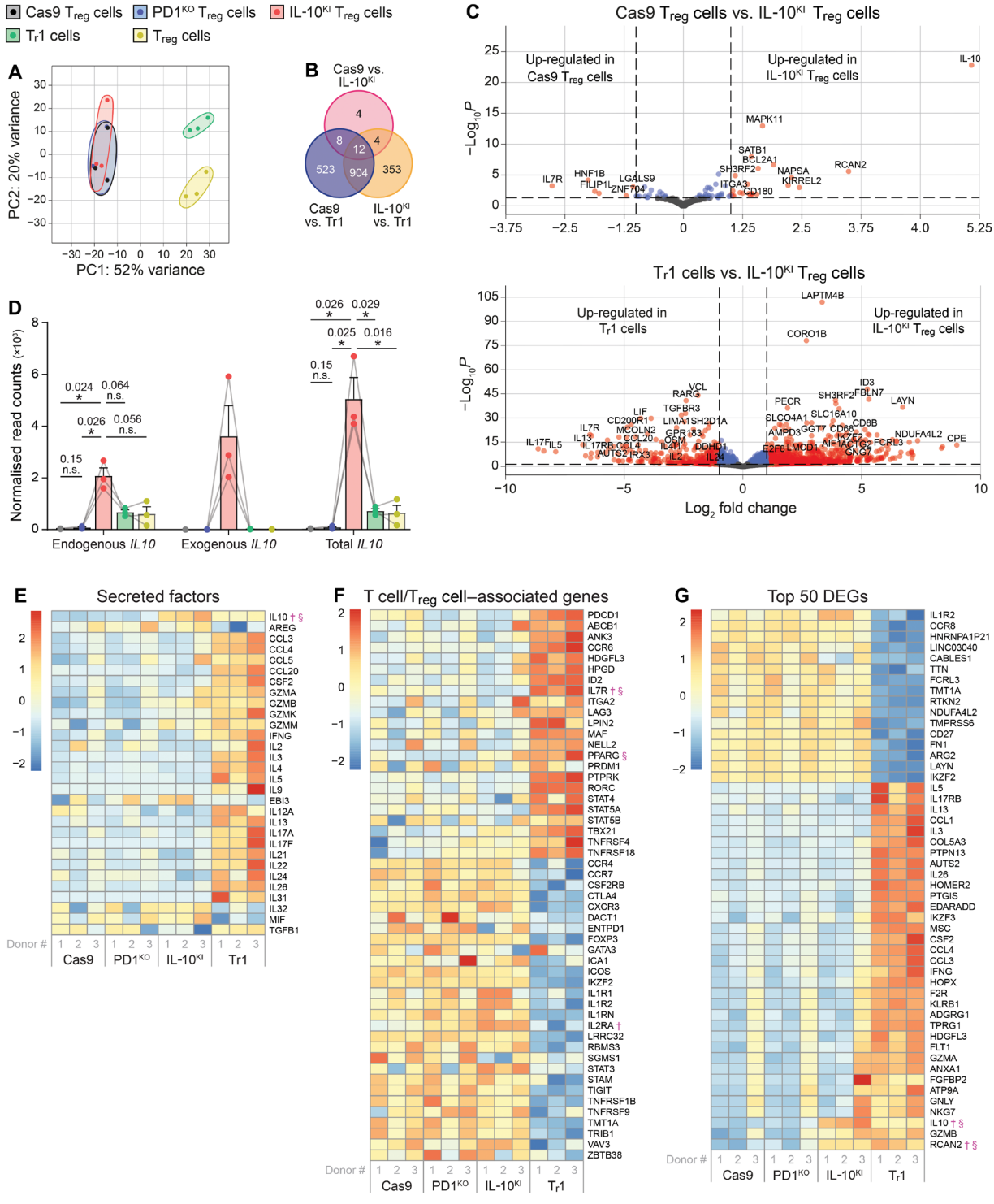

Fig. 3. IL-10^{KI} T$_{reg}$ cells retain their characteristic transcriptome, which is distinct from T$_r$1 cells. A2-CAR T$_{reg}$ cell types, A2-CAR T$_r$1 cells and A2-CAR T$_{conv}$ cells were stimulated with HLA-A2$^+$ beads for 16 hours, then RNA was extracted and analyzed. (**A**) Principal component analysis. PC, principal component. (**B**) Venn diagram showing the total number of significantly up- and down-regulated genes in each comparison. (**C**) Volcano plots showing differential gene expression of Cas9 versus IL-10^{KI} T$_{reg}$ cells (top) and IL-10^{KI} T$_{reg}$ cells versus T$_r$1 cells (bottom). [(B) and (C)] Significant DEGs were identified on the basis of $P < 0.05$ and a $\log_2$ fold change of 1. (**D**) Normalized read counts of endogenous, exogenous, and total (endogenous + exogenous) *IL10* transcripts. Data are means ± SEM with data points from individual subjects connected ($n = 3$). (**E** to **G**) Heatmaps showing the relative expression of (E) select secreted factors, (F) T cell/T$_{reg}$ cell–associated genes, and (G) the top 50 DEGs in an IL-10^{KI} T$_{reg}$ cell versus T$_r$1 cell comparison. [(E) to (G)] Statistical significance was determined using a Wald test with Benjamini-Hochberg correction. No DEGs with $P < 0.05$ for Cas9 versus PD1^{KO} T$_{reg}$ cells. †$P < 0.05$ for Cas9 versus IL-10^{KI} T$_{reg}$ cells. §$P < 0.05$ for PD1^{KO} versus IL-10^{KI} T$_{reg}$ cells. n.s., not significant.

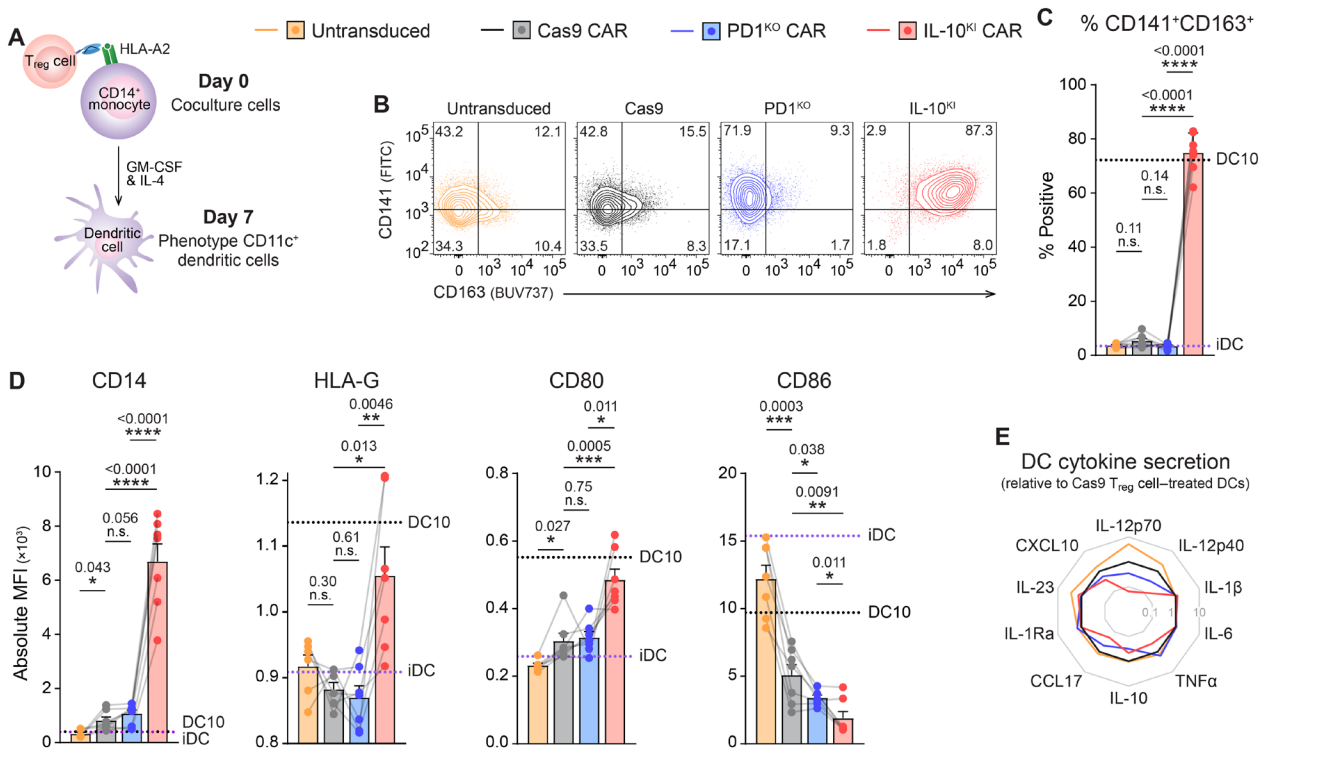

Fig. 4. IL-10^{KI} T$_{reg}$ cells promote differentiation of DCs with a DC10-like phenotype. (**A**) Schematic diagram of experiment. CD14^{+}HLA-A2^{+} cells were differentiated into dendritic cells (DCs) with GM-CSF (100 ng/ml) and IL-4 (10 ng/ml), in the absence (iDC) or in the presence of the indicated types of A2-CAR T$_{reg}$ cells (10:1 monocyte:T$_{reg}$ cell ratio), or with rIL-10 (DC10). After 7 days, the DC phenotype was analyzed. (**B**) Representative and (**C**) averaged data showing expression of CD163 and CD141 in live CD11c^{+}CD4^{-} DCs. (**D**) Expression of tolerogenic markers in live CD11c^{+}CD4^{-} DCs, with data from control iDC or DC10 represented with purple and black dotted lines, respectively. (**E**) In some experiments, CD11c^{+}CD4^{-} DCs were sorted at the end of the 7-day coculture and stimulated with LPS and IFN-γ for 48 hours, and supernatants were analyzed for the indicated cytokines. Cytokine secretion data are shown relative to DCs treated with Cas9 A2-CAR T$_{reg}$ cells. Averaged data are means ± SEM with connecting data points from individual subjects (n = 5 to 7). Statistical significance was determined using mixed-effects analysis tests with P values shown. n.s., not significant.

alloreactive CD4^{+} T cell proliferation significantly more effectively than all other T$_{reg}$ cell conditions analyzed (Fig. 6, B and C).

To further confirm the enhanced suppressive function of IL-10^{KI} T$_{reg}$ cells, we performed a second APC-dependent suppression assay where the ability of T$_{reg}$ cells to inhibit autoreactive islet-specific CD4^{+} T cells was tested (Fig. 6D). CD4^{+} responder T cells were transduced to express an islet autoantigen–specific TCR, specifically the 4.13-TCR (*29*), which recognizes glutamic acid decarboxylase 65 (GAD65) peptide presented in the context of HLA-DR4 (Fig. 6E). T$_{reg}$ cells were cocultured with HLA-A2^{+}HLA-DR4^{+} DCs, and the subsequent ability of these DCs to stimulate 4.13-TCR^{+} responder T cells in the presence of GAD65 peptide was assessed (Fig. 6D). CD4^{+} responder T cell proliferation was measured by the induced expression of Ki67, a well-established proliferation marker. Similar to observations with alloreactive T cells, Cas9, and PD1^{KO} T$_{reg}$ cells exhibited a comparable level of suppression, while IL-10^{KI} T$_{reg}$ cells inhibited Ki67 expression in autoreactive responder T cells significantly more effectively (Fig. 6, F and G). Analysis of the supernatants from these suppression assays also revealed that cultures containing IL-10^{KI} T$_{reg}$ cells had significantly less pro-inflammatory cytokines (PD1^{KO} versus IL-10^{KI} IL-2, P = 0.024, and IL-6, P = 0.011; Fig. 6H). Overall, these results show that IL-10^{KI} T$_{reg}$ cells are superior to Cas9/PD1^{KO} T$_{reg}$ cells and have an enhanced ability to suppress allo- and autoreactive T cells.

PD1 deletion and IL-10^{KI} do not compromise T$_{reg}$ cell lineage stability

It has previously been suggested that overstimulation of T$_{reg}$ cells can drive instability and identity loss (*41*). To test whether PD1^{KO} and IL-10^{KI} T$_{reg}$ cells maintained expression of FOXP3 and Helios in an in vivo chronic CAR stimulation setting, cells were injected into NOD.Cg-*Prkdc*^{scid}*Il2rg*^{tm1Wjl}/SzJ (NSG) mice that ubiquitously expressed HLA-A2 (A2-NSG), together with an equal number of autologous PBMCs (Fig. 7A). After 3 weeks, the T$_{reg}$ cells were re-isolated and analyzed by flow cytometry. Cas9, PD1^{KO}, and IL-10^{KI} T$_{reg}$ cells all maintained high expression of FOXP3 and Helios, indicating no loss of stability upon chronic CAR stimulation (Fig. 7B). This conclusion was further confirmed by analyzing the *FOXP3* methylation status in T$_{reg}$ cells that were sorted from mouse spleens. Levels of methylation in the T$_{reg}$ cell–specific demethylation region (TSDR) revealed no differences between Cas9, PD1^{KO}, and IL-10^{KI} cells (Fig. 7C). Overall, these results demonstrate that PD1-ablation and *IL10* integration into the *PDCD1* locus did not affect T$_{reg}$ cell lineage stability.

IL-10^{KI} T$_{reg}$ cells are safe, secrete IL-10, and suppress mouse DCs in a xenoGVHD model

To investigate the safety and efficacy of IL-10^{KI} CAR T$_{reg}$ cells in vivo, xenogeneic graft-versus-host-disease (xenoGVHD) experiments were performed where NSG mice were administered

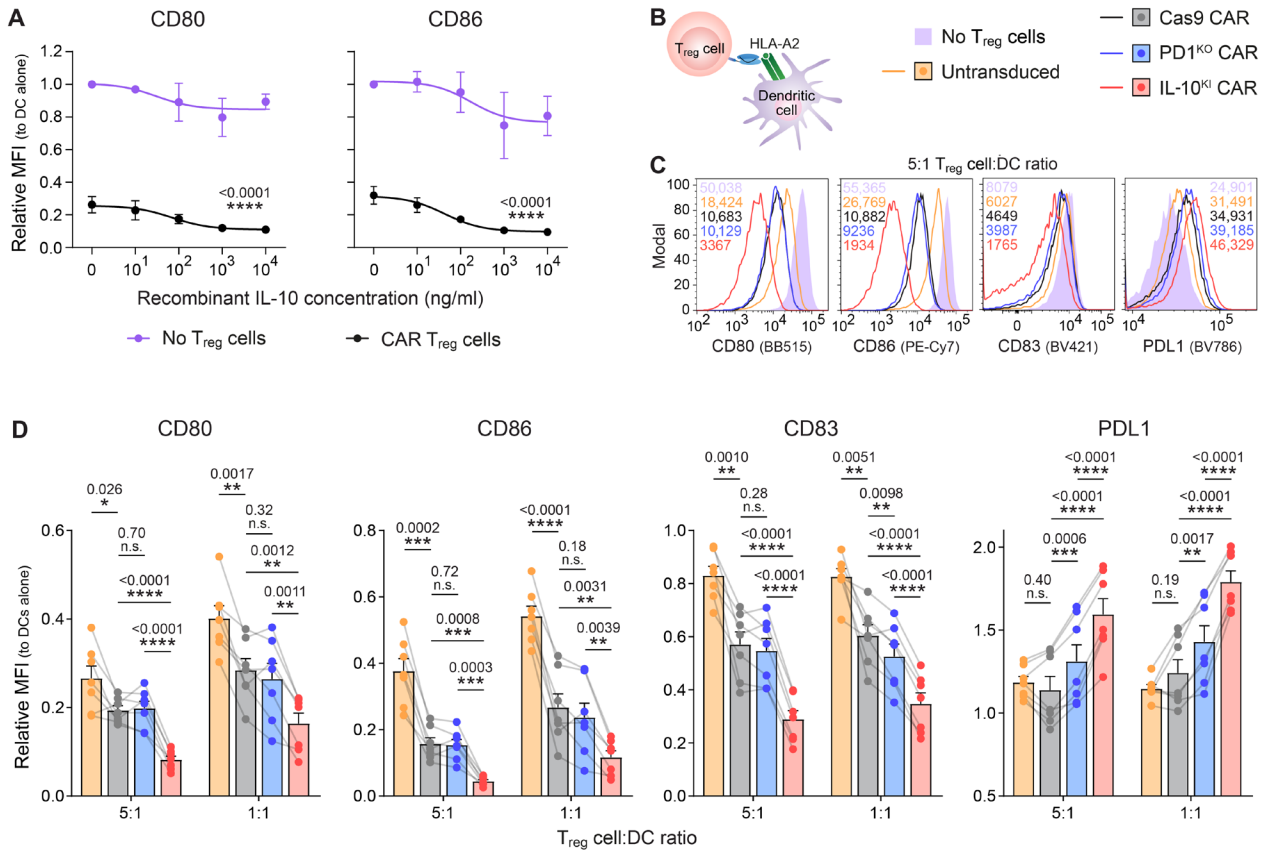

Fig. 5. IL-10^{KI} T$_{reg}$ cells induce a tolerogenic phenotype in mDCs. (**A**) HLA-A2^{+} mDCs were cultured with varying amounts of rIL-10, in the presence or absence of A2-CAR T$_{reg}$ cells (not CRISPR modified), and, after 72 hours, CD80 and CD86 expression was measured. Statistical significance indicates mixed-effects analysis only of the CAR T$_{reg}$ cell–treated DCs condition (**B**) Schematic diagram of DC suppression assay. mDCs were cocultured with different types of A2-CAR T$_{reg}$ cells for 72 hours, after which expression of co-stimulatory/inhibitory molecules on live CD11c^{+}CD4^{-} cells was measured. (**C**) Representative and (**D**) pooled data showing relative MFIs compared to mDCs that were cultured without T$_{reg}$ cells. Averaged data are means ± SEM with connecting data points from individual subjects (n = 3 to 7). Statistical significance was determined using mixed-effects analysis tests without (A) or with (D) Fisher's multiple comparisons test, with P values shown. n.s., not significant.

HLA-A2^{pos}CD4^{+} T$_{conv}$ cells without or with different ratios of Cas9 or IL-10^{KI} A2-CAR T$_{reg}$ cells (Fig. 8A). Mice were regularly scored for xenoGVHD and euthanized when predefined endpoint criteria were met. In a first experiment, T$_{reg}$ cells were co-infused at a 1:1 or 1:2 T$_{reg}$ cell:T$_{conv}$ cell ratio (Fig. 8, B to D). Consistent with previous data (*5*, *8*), Cas9 T$_{reg}$ cells potently suppressed xenoGVHD, and IL-10^{KI} T$_{reg}$ cells were similarly effective, with no evidence of deleterious effects of the IL-10^{KI} T$_{reg}$ cells (Fig. 8B). Engraftment of HLA-A2^{pos} T$_{conv}$ cells and HLA-A2^{neg} T$_{reg}$ cells was monitored in peripheral blood (Fig. 8C), revealing that, on day 28 in the 1:1 ratio condition, IL-10^{KI} T$_{reg}$ cells suppressed T$_{conv}$ cell engraftment more effectively than Cas9 T$_{reg}$ cells. IL-10^{KI} T$_{reg}$ cells also had a trend toward greater engraftment persistence. Analysis of plasma confirmed that the IL-10^{KI} T$_{reg}$ cells secreted significant quantities of IL-10. Cas9 and IL-10^{KI} T$_{reg}$ cells suppressed T$_{conv}$ cell secretion of IFN-γ to a similar degree (Fig. 8D).

In the above xenoGVHD model, human APCs do not engraft, so we took advantage of the fact that human IL-10 is functional on mouse cells (*42*) and, in a second experiment, investigated whether IL-10^{KI} T$_{reg}$ cells influenced the phenotype of tissue-resident mouse APCs. Cas9 and IL-10^{KI} T$_{reg}$ cells were infused at a 1:4 T$_{reg}$ cell:T$_{conv}$ cell ratio (Fig. 8E). After 7 weeks, immune cells were isolated from the intestine and ear skin. We found that mouse CD11c^{+} cells expressed significantly lower levels of major histocompatibility complex (MHC) class I (H-2Kd), MHC class II (I-Ag7), and CD86 when treated with IL-10^{KI} T$_{reg}$ cells, compared to Cas9 T$_{reg}$ cells (Fig. 8E), confirming that the IL-10 present in the plasma of these IL-10^{KI} T$_{reg}$ cell–treated mice was functional. Overall, these results demonstrate that IL-10^{KI} T$_{reg}$ cells suppress xenoGVHD, are well tolerated, and secrete amounts of IL-10 that are able to suppress APCs in vivo.

DISCUSSION

In this study, we built on the concept of using CAR T$_{reg}$ cells as an immunoregulatory cell therapy product and created so-called "armored" CAR T$_{reg}$ cells that were engineered to simultaneously remove an inhibitory signal and enhance a suppressive mechanism. Using PD1 as a representative inhibitory molecule and IL-10 as a prototypical suppressive cytokine, we demonstrated that the function of CAR T$_{reg}$ cells can be substantially increased by replacing *PDCD1* with *IL10*. Working in the human system with an A2-CAR, we found that IL-10^{KI} T$_{reg}$ cells took on advantageous properties of Tr1 cells, adopting an enhanced ability to drive tolerogenic DC development and control both allo- and autoreactive T cells in vitro.

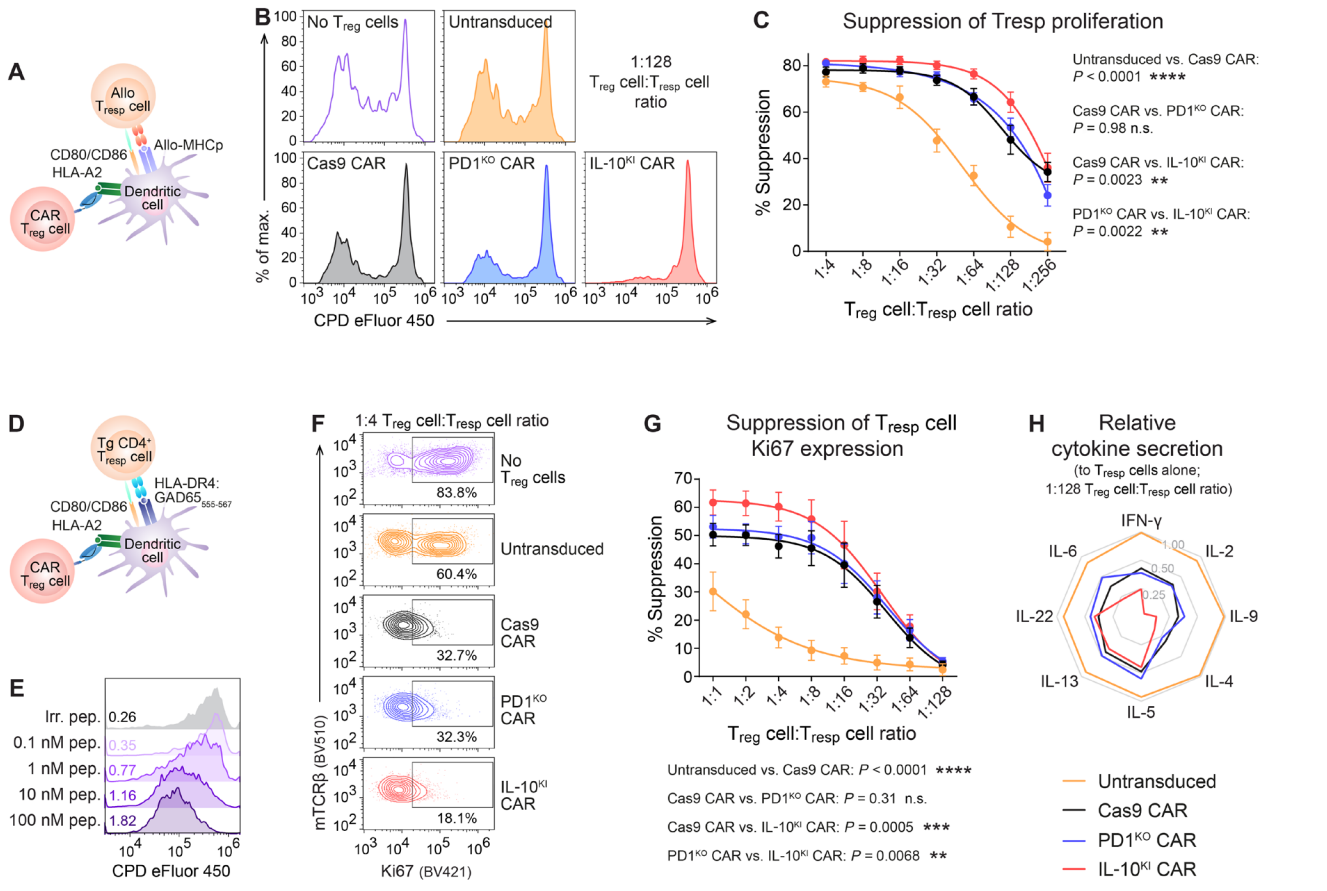

Fig. 6. IL-10^{KI} CAR T$_{reg}$ cells suppress alloantigen- and autoantigen-specific T cell proliferation. (**A**) Schematic diagram of alloantigen-based suppression assay shown in (B) and (C). HLA-A2$^+$ DCs were cocultured with HLA-A3$^-$ T$_{reg}$ cells for 72 hours. Allogeneic CPD eFluor 450–labeled HLA-A3$^+$CD3$^+$ responder T cells were then added, and cocultures were maintained for an additional 96 hours. (**B**) Representative CD4$^+$ responder T cell proliferation, gated on live HLA-A3$^+$CPD eFluor 670$^-$CPD eFluor 450$^+$CD4$^+$ cells. (**C**) % Suppression of CD4$^+$ responder T cell proliferation, relative to responder T cells cultured without T$_{reg}$ cells. (**D**) Schematic diagram of islet antigen–based suppression assay shown in (F) to (H). HLA-A2$^+$HLA-DR4$^+$ DCs were cocultured with T$_{reg}$ cells for 48 hours. CD4$^+$4.13-TCR$^+$ responder T cells and 1 nM GAD65 peptide were then added, and cocultures were maintained for an additional 48 hours. (**E**) CD4$^+$4.13-TCR$^+$ T cell proliferation following 96-hour coculture with immature HLA-DR4$^+$ DCs and varying GAD65 peptide concentrations (without T$_{reg}$ cells). Control cells were pulsed with an irrelevant hemagglutinin peptide (100 nM). Division indices provided. (**F**) Representative CD4$^+$ responder T cell proliferation, gated on live CD4$^+$CPD eFluor 670$^-$mTCRβ$^+$ cells. (**G**) % Suppression of responder T cell proliferation, relative to responder T cells stimulated without T$_{reg}$ cells. (**H**) Relative cytokine analysis from 1:128 T$_{reg}$ cell:responder T cell (T$_{resp}$ cell) ratio. TNFα, IL-17A & IL-17F were not detected. Averaged data are means ± SEM with non-linear regression lines (n = 8 to 10). Statistical significance was determined using mixed-effects analysis with P values shown. n.s., not significant.

This was achieved without the induction of pro-inflammatory cytokine secretion, in contrast to T$_r$1 cells (*26*, *43*). IL-10^{KI} T$_{reg}$ cells also remained stable upon adoptive transfer into A2-NSG mice and were safe and effective in a xenoGVHD model. To our knowledge, these findings are the first to demonstrate the benefits of using genome engineering to enhance a functional pathway in CAR T$_{reg}$ cells and create cells with "hybrid" functions that are usually present in two distinct cell types.

Seeking antigen-dependent control of a functionally advantageous transgene, we chose to target the *PDCD1* locus as PD1 expression is activation induced (*11*) and there is the added benefit that PD1 signaling is deleterious for T$_{reg}$ cell activation (*8*, *16*, *17*). Although some studies found that PD1 signaling promotes FOXP3 expression and conversion of T cells into T$_{reg}$ cells (*44*–*47*), most studies concluded that PD1 signaling in established T$_{reg}$ cells is detrimental for their function (*8*, *16*, *18*, *22*, *23*). In our study, CRISPR-mediated PD1 ablation increased the activation potential of CAR T$_{reg}$ cells but, unlike cancer-relevant CAR-T cells (*48*, *49*), this modification did not significantly improve their function. This could be due to the strong benefits of CAR expression dominating any functional advantage of PD1 deletion. PD1 ablation did not compromise T$_{reg}$ cell stability or diminish their function in any DC- or T cell–directed assay.

Given that PD1 is transiently expressed upon stimulation in non-exhausted cells, various cancer immunotherapy studies have explored the advantages of exploiting the *PDCD1* locus to regulate expression of exogenous transgenes. Insertion of an anti-CD19 CAR into the *PDCD1* locus of T cells using a nonviral gene editing strategy was shown to reduce CAR-T cell exhaustion upon repetitive in vitro stimulation (*50*), and the therapeutic efficacy of these cells was confirmed in a phase 1 clinical trial (*15*). In our study, we modified this strategy to insert a functionally relevant transgene into the *PDCD1*

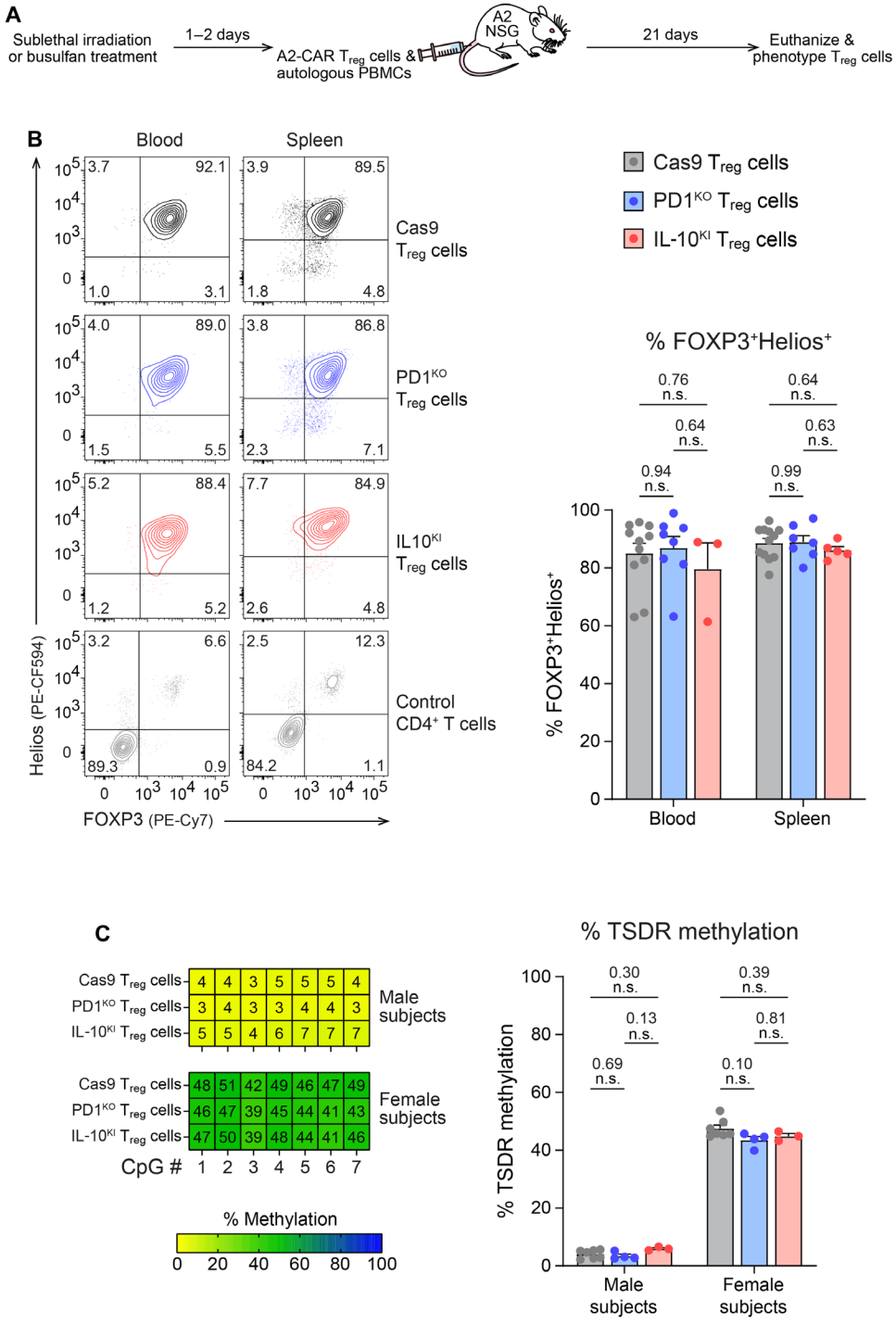

Fig. 7. PD1^{KO} and IL-10^{KI} T_{reg} cells maintain their stability following chronic, in vivo CAR stimulation. (**A**) Schematic diagram of model. 1.5 to 3.2 million A2-CAR T_{reg} cells were coadministered with an equal number of autologous PBMCs into preconditioned A2-NSG mice. Mice were euthanized after 21 days. (**B**) FOXP3 and Helios expression in hCD45$^+$mCD45$^-$hCD4$^+$cMyc$^+$ T_{reg} cells in blood or spleen. FOXP3 and Helios gates were set on hCD4$^+$ cells in mice reconstituted with PBMCs alone. (**C**) Upon euthanasia, hCD45$^+$mCD45$^-$hCD4$^+$cMyc$^+$ T_{reg} cells were isolated from splenocytes by cell sorting. Data show the methylation status of the TSDR locus in the sorted T_{reg} cells. Averaged data are means ± SEM with connecting data points from individual subjects (n = 3 to 5). Statistical significance was determined using one-way analysis of variance (ANOVA) with P values shown. n.s., not significant.

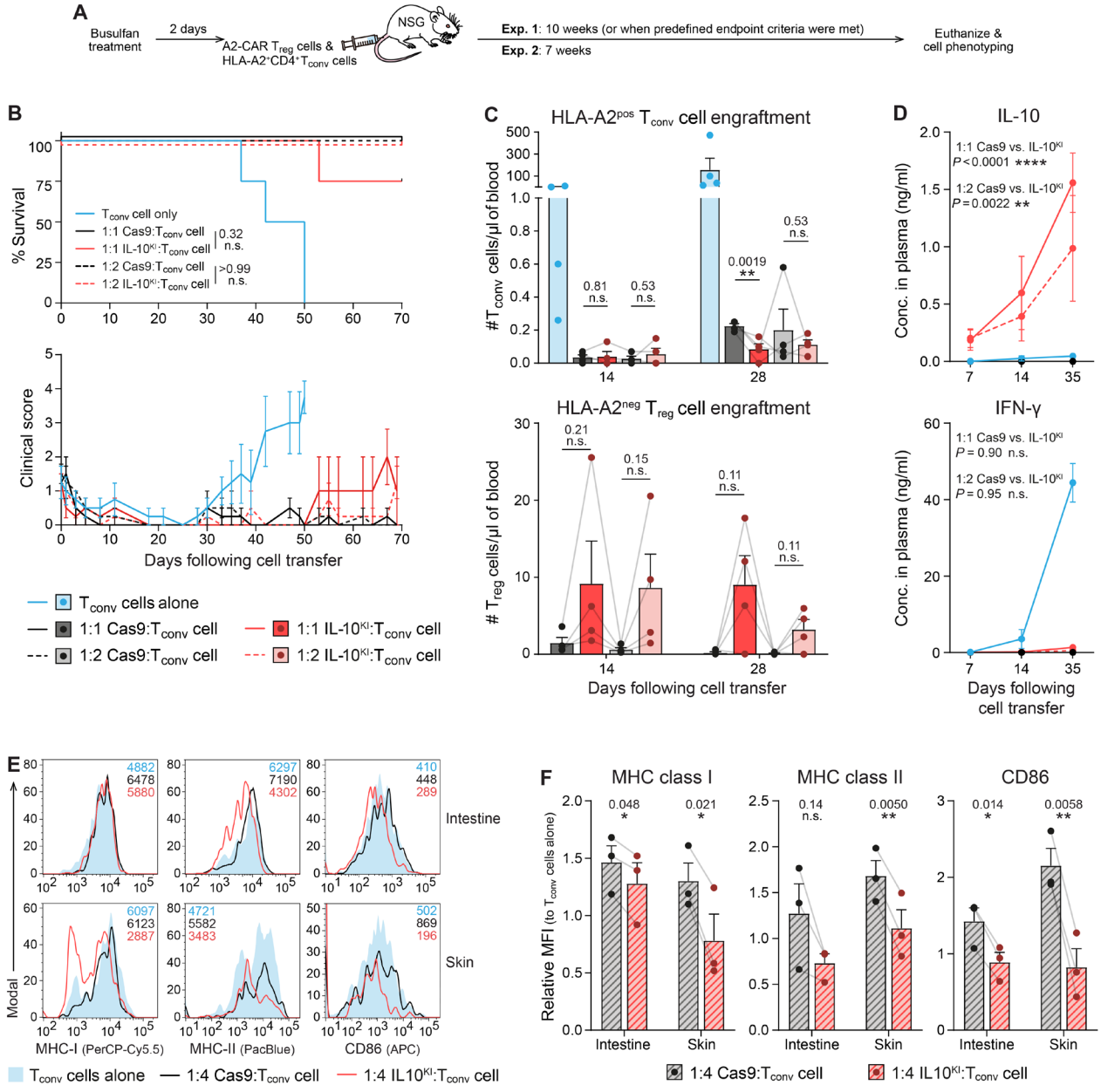

Fig. 8. IL-10^{KI} T$_{reg}$ cells secrete IL-10 in vivo and suppress DCs and xenoGVHD. (**A**) Schematic diagram of model. Preconditioned NSG mice were intravenously administered HLA-A2^{neg} A2-CAR T$_{reg}$ cell types and HLA-A2^{pos}CD4$^+$ T$_{conv}$ cells at T$_{reg}$ cell:T$_{conv}$ cell ratios of (B to D) 1:1, 1:2, or (E and F) 1:4. Mice were monitored and euthanized at 7 or 10 weeks after cell transfer, or when predefined endpoint criteria were met. (**B**) % Survival (top) and clinical scores (bottom) following cell transfer. (**C**) Absolute numbers of HLA-A2^{pos} T$_{conv}$ cells (top) and HLA-A2^{neg} T$_{reg}$ cells (bottom) in peripheral blood at days 14 and 28. (**D**) Quantities of human IL-10 (top) and IFN-γ (bottom) in mouse plasma over time. Other cytokines (IL-2, IL-4, IL-5, IL-6, IL-9, IL-13, IL-17A, IL-17F, IL-22, and TNFα) were not detected. (**E** and **F**) (E) Representative and (F) averaged data showing the phenotype of mouse CD45$^+$CD11c$^+$ cells isolated from the intestine or ear skin, 7 weeks after cell injection. Representative plots show the MFI of NOD mouse MHC class I (H-2Kd), MHC class II (I-Ag7), and CD86. Averaged data are means ± SEM with each point representing one mouse (n = 3 to 4). For each group, mice were administered T$_{reg}$ cells that were isolated from a different human subject; connecting data points represent each individual subject. Statistical significance was determined using a log-rank Mantel-Cox test (B), paired two-tailed Student's t tests [(C) and (F)], or two-way ANOVA (D) with P values shown. n.s., not significant.

locus, yielding a T$_{reg}$ cell product that constitutively expressed an HLA-A2–specific CAR and expressed the immunosuppressive cytokine IL-10 in response to antigen stimulation. Using a similar gene editing strategy, Kim *et al.* (*51*) also observed activation-dependent expression in their cancer-based study that inserted IL-12 into the *PDCD1* locus of TCR-edited NY-ESO T cells. The SynNotch system has also recently been used to generate T cells that secrete IL-10 in response to antigen engagement, yielding a T$_{conv}$ cell–based product that can suppress EAE (*52*).

T$_{reg}$ cells are known to exert their immunosuppressive function by using a variety of mechanisms, but the relevance of each pathway in different disease contexts remains relatively uncharacterized. We

selected IL-10 as an ideal candidate for enhancing the suppressive function of T_{reg} cells as it is a well-established immunoregulatory cytokine that is secreted at relatively low levels compared to T_r1 cells (*26*). IL-10 therapy has been investigated clinically as a monotherapy (*53*, *54*), but its short half-life is thought to have limited the levels of IL-10 present in the required tissues (*55*). IL-10 primarily achieves its immunosuppressive effect by acting on myeloid cells. Although it can act directly on T cells, it counters co-stimulatory signals (particularly CD28 signaling) and not TCR or IL-2–mediated signaling cascades (*37*, *38*). Moreover, we found that resting T cells express low levels of the IL-10R, consistent with previous reports (*39*). Collectively, these findings offer an explanation for the modest functional advantage of IL-10^{KI} in APC-independent suppression assays.

A clear advantage of editing CAR T_{reg} cells to express IL-10 instead of using CAR T_r1 cells is the low amounts of pro-inflammatory cytokines produced by the former. The concept of endowing CAR T_{reg} cells with constitutive IL-10 expression has been explored, with mixed results (*32*, *56*). Constitutive IL-10 expression slightly increased the suppressive function of human A2-CAR T_{reg} cells in a CAR-dependent suppression assay (*32*) but had no advantage for mouse CAR T_{reg} cells specific for factor VIII (*56*). Constitutive IL-10 secretion by human epidermal growth factor receptor 2 (HER2)-specific CAR T cells has been shown to be beneficial in an oncology setting, as these cells are better protected from mitochondrial dysfunction (*57*). In contrast to IL-10^{KI} T_{reg} cells, we found that T_{reg} cells constitutively secreting IL-10 exerted CAR-independent suppression (fig. S4B). Antigen-independent IL-10 secretion could be deleterious in vivo as it could promote pan-immunosuppression or possibly inflammation given the pleiotropic effects of IL-10 on $CD8^+$ T cell expansion and B cell antibody secretion (*58*–*61*). Our strategy reduces this concern as IL-10 is secreted in an activation-dependent manner. Emerging protein engineering strategies that improve the binding of IL-10 to its cognate receptor could also be adapted for use in T_{reg} cells to reduce any inflammatory effects of native IL-10 (*62*, *63*).

Confirming the functional potency of IL-10^{KI} T_{reg} cells on in vitro T cell proliferation was challenging as, in the typical polyclonal suppression assay, responder T cells are stimulated with artificial anti-CD3/CD28 beads. As such, this APC-independent system does not effectively mimic endogenous T cell stimulation. The paucity of humanized mouse models in which pathology is driven by human T cell–APC interactions similarly limited our testing of IL-10^{KI} T_{reg} cells in vivo. Using a xenoGVHD model, we confirmed that IL-10^{KI} T_{reg} cells secreted IL-10 and were effective and safe in vivo. In this model, CAR expression potently stimulates T_{reg} cell suppression, resulting in complete protection without or with IL-10. Although human APCs were not present in this model, we found that IL-10^{KI} T_{reg} cells had significant effects on mouse $CD11c^+$ DCs, with down-regulated expression of MHC classes I and II and CD86. Notably, this was evident in intestinal and skin tissues, two locations where local IL-10 expression by therapeutic cells could be highly beneficial.

One consideration regarding the translatability of our findings is the logistical complexity of introducing three genetic modifications using lentivirus and CRIPSR editing. We opted to use AAV6 to deliver an HDRT encoding the IL-10 transgene into T_{reg} cells, but future studies should consider using nonviral gene delivery systems to decrease the cost, complexity, and potential immunogenicity of AAV6 (*50*, *64*, *65*). Another general concern in the CAR T_{reg} cell field is the question of whether these cells could inadvertently inhibit desired immune responses (e.g. prevent clearance of infections or limit antitumor immunity). While studies have shown that engineering CAR T cells to express IL-10 can be advantageous for antitumor immunity (*57*), investigation of how this finding applies to therapeutic T_{reg} cells is warranted. Engineering cell therapy products with safety switches may be a partial solution, but further studies are required to comprehensively address this issue.

Overall, this study shows the potential of gene engineering to enhance the therapeutic potency of CAR T_{reg} cells. Although IL-10 secretion is often cited as a key T_{reg} cell mechanism of action, critically important for immune regulation in tissues at environmental interfaces (*66*), its expression is low in human T_{reg} cells isolated from blood (*26*). Thus, blood-derived T_{reg} cells tested in clinical trials to date have likely had low IL-10 expression. Our data show that this pathway can be introduced ectopically to significantly improve T_{reg} cell function, without loss of lineage stability. The findings set the stage for using this strategy to make T_{reg} cells with enhanced therapeutic effects for multiple applications in transplantation and autoimmunity. Other immunoregulatory or tissue reparative molecules could similarly be incorporated into the *PDCD1* or other antigen-stimulated loci to improve CAR T_{reg} cell function.

MATERIALS AND METHODS

Study design

The objectives of this study were to address the following predetermined hypotheses: (i) CRISPR-mediated removal of PD1 would allow human CAR T_{reg} cells to achieve a higher activation state in response to a specific CAR stimulant; (ii) the *PDCD1* locus could be exploited to facilitate activation-induced expression of an IL-10 transgene; and (iii) replacing *PDCD1* with *IL10* would enhance the suppressive potency of human CAR T_{reg} cells. Experiments were performed using cells isolated from the peripheral blood of anonymized human subjects. Male and female subjects were segregated by sex for T_{reg} cell stability experiments in which TSDR analyses were performed (Fig. 7). For all other experiments, subjects were not stratified according to sex. Within each experiment, Cas9, PD1^{KO}, and IL-10^{KI} T_{reg} cells (as well as T_r1 and T_{conv} cells) were generated from the same subject to reduce donor-to-donor variability; the relative contribution of each subject is shown with connected points. Experiments were performed at least twice with two to four individual subjects per experiment; the number of biological replicates is stated in the figure legends, and sample sizes were established before performing the experiments on the basis of our previous experience with similar experimental approaches to achieve statistical significance.

Cytokine secretion values regarded as "not detectable" were excluded from analyses if the predicted concentrations were below the LEGENDPlex (BioLegend) threshold of detection and/or consistently <1 pg/ml for multiple donors. For flow cytometry data, median fluorescence intensity (MFI) values were excluded from final analyses if they were based on <50 gated events (relevant only to in vivo data). No other data were excluded from our analyses.

Subjects, mice, and ethical approvals

Peripheral blood in the form of buffy coat products was obtained from anonymized healthy adults via Canadian Blood Services (Vancouver, BC, Canada) with informed consent and ethical approval from The University of British Columbia Clinical and Canadian

Blood Service Research Ethics Boards (H18-02553). NSG (JAX, no. 005557) mice and transgenic NSG mice that ubiquitously express HLA-A2 (A2-NSG; JAX, no. 014570; both from the Jackson Laboratory) were bred in-house and maintained under specific pathogen–free conditions. All in vivo experiments were carried out in accordance with the National Research Council's *Guide for the Care and Use of Laboratory Animals* using protocols approved by The University of British Columbia Animal Care Committee (A22-0120).

Molecular biology and vector synthesis

HDRTs were designed with ~800–base pair (bp) homology arms to insert designated sequences into the *PDCD1* locus following CRISPR-mediated cutting with crRNA3. An *IL10-tCD19* ORF was gene synthesized (GeneArt) and cloned by Gibson assembly (New England Biolabs, NEB) into an AAV6 transfer plasmid (*67*), thereby generating pssAAV_PDCD1cr3.HDRT-IL10tCD19 (Fig. 1B, right). The IL-10–encoding sequence was then removed to generate pssAAV_PDCD1cr3.HDRT-tCD19 (Fig. 1B, left).

pCCL_A2CAR-tNGFR and pCCL_HLAA2-eGFP were generated as previously described (*5*). pCCL_wtIL10-tNGFR, pCCL_MQIPQ-IL10-tNGFR, and pCCL_wtIL10-tCD19 were generated by amplifying *IL10* from the pssAAV_PDCD1cr3.HDRT-IL10tCD19 vector and inserting this polymerase chain reaction (PCR) product into either an empty pCCL_tNGFR or pCCL_tCD19 target vector. pELNS_PDL1 was generated by cloning PCR-amplified *PDL1* cDNA (Sino Biological) into the pELNS vector using Gibson assembly. pCCL_4.13TCR-tNGFR was generated by replacing the *A2CAR* cDNA in the pCCL_A2CAR-tNGFR vector with 4.13TCRα and 4.13TCRβ-chain sequences (*29*) that were split by a P2A sequence. TCR constant regions were replaced with mouse TCR α constant (TRAC) and TCR β constant (TRBC) sequences to allow identification of transduced cells. All vectors were validated by restriction digest and Sanger sequencing before use.

Cell line culture

Human embryonic kidney (HEK) 293T clone 17 cells [American Type Culture Collection (ATCC), no. CRL-11268] were cultured in Iscove's modified Dulbecco's medium (IMDM) supplemented with 10% fetal bovine serum (FBS), penicillin-streptomycin (100 U/ml), and 2 mM GlutaMAX (all from Thermo Fisher Scientific). L cells expressing human CD32, CD58, and CD80 (*68*) were cultured in Roswell Park Memorial Institute (RPMI) 1640 (Thermo Fisher Scientific) supplemented with 10% FBS (Hyclone Laboratories Inc.), penicillin-streptomycin (100 U/ml), and 2 mM GlutaMAX. HLA-$A2^+$ L cell derivatives were generated by lentivirally transducing $CD32^+CD58^+CD80^+$ L cells with pCCL_HLAA2-eGFP. Cells were passaged by washing with phosphate-buffered saline (PBS), incubating with 0.05% trypsin-EDTA (Thermo Fisher Scientific) for 2 to 3 min and neutralizing with cell culture medium.

K562 cells (ATCC, no. CRL-3343) were cultured in RPMI 1640 supplemented with 10% FBS, penicillin-streptomycin (100 U/ml), and 2 mM GlutaMAX. HLA-$A2^+$PD-$L1^-$ and HLA-$A2^+$PD-$L1^+$ K562 derivatives were generated by lentivirally transducing blank K562s with pCCL_HLAA2-eGFP and pELNS_PDL1.

Virus production

To generate lentiviral particles, HEK293T/17 cells were transfected with either (i) pCCL_A2CAR-tNGFR, (ii) pCCL_wtIL10-tCD19, (iii) pCCL_4.13TCR-tNGFR, (iv) pCCL_HLAA2-eGFP, or (v) pELNS_PDL1, and a mixture of pRSV-REV, pMDLG/pRRE, pMD2.g, and pAdVAntage Vector (further details on addgene.org) using calcium phosphate (made in-house). Cell supernatants were harvested 45 to 48 hours post-transfection, and lentiviral particles were concentrated by ultracentrifugation at 76,755*g*. Viral titers were calculated by limiting dilution transduction of HEK293T/17 cells, and virus aliquots were stored at −80°C.

To generate AAV6 viral particles, HEK293T/17 cells were co-transfected with either pssAAV_PDCD1cr3.HDRT-tCD19 or pssAAV_PDCD1cr3.HDRT-IL10tCD19 and a mixture of pHelper and pAAV6-Rep-Cap (both from Cell Biolabs) using calcium phosphate. Culture supernatants were replenished after 12 to 16 hours and harvested ~68 hours post-transfection. AAV6 particles were concentrated using the AAVpro Purification Kit, quantified using the AAVpro quantification kit (both from Takara Bio) and stored at −80°C.

RNP generation

PDCD1-targeting crRNA1 (5′-CGTCTGGGCGGTGCTACAACTGG-3′) (*69*–*71*), crRNA2 (5′-GGCCAGGATGGTTCTTAGGTAGG-3′) (*70*, *72*), and crRNA3 (5′-CGACTGGCCAGGGCGCCTGTGGG-3′) (*49*, *73*–*75*) were reconstituted at 200 μM in nuclease-free Duplex buffer and duplexed at a 1:1 molar ratio with tracrRNA (all from Integrated DNA Technologies, IDT) by heating to 95°C for 5 min and cooling to room temperature, as previously described (*67*). Resulting gRNA was then combined at a 2:1 molar ratio with Cas9-NLS (nuclear localization signal) protein (QB3 MacroLab) and incubated for 10 min at room temperature to generate RNPs. RNPs were used immediately or stored at −80°C. Each electroporation contained $<2 \times 10^5$ cells and 20 pmol of Cas9 ± 40 pmol of gRNA in a total volume of 10 μl.

T_{reg} cell isolation, gene editing, and expansion

$CD4^+$ T cells were enriched from peripheral blood of HLA-$A2^-$ subjects using the RosetteSep Human $CD4^+$ T Cell Enrichment Cocktail (STEMCELL Technologies), and $CD25^+$ cells were separated using CD25 MicroBeads II (Miltenyi Biotec). Naïve $CD4^+CD25^{hi}CD127^{lo}CD45RA^+CD45RO^-$ T_{reg} cells and naïve $CD4^+CD25^-CD127^+CD45RA^+CD45RO^-$ T_{conv} cells were then purified by cell sorting. Sorted T cells were stimulated with artificial APCs [L cells expressing human CD32, CD58, and CD80; irradiated with 7500 centigray (cGy)] loaded with anti-CD3 monoclonal antibody (OKT3, UBC AbLab) and cultured in ImmunoCult XF (STEMCELL Technologies) supplemented with penicillin-streptomycin (100 U/ml). T_{reg} cells and T_{conv} cells were cultured with recombinant human IL-2 at 1000 and 100 IU/ml, respectively (Proleukin, Prometheus Laboratories Inc.).

T_{reg} cells were transduced with the A2-CAR construct 24 hours poststimulation using lentivirus at a multiplicity of infection of 10, as previously described (*5*). On day 5, T_{reg} cells were CRISPR-edited using the Neon Transfection System 10-μl Kit (Thermo Fisher Scientific) and restimulated, as previously described (*67*). Briefly, T_{reg} cells were harvested, washed twice with PBS, and resuspended in Buffer T ($<2 \times 10^5$ cells/10 μl) containing Cas9 or complexed RNPs. Cells were then electroporated in one pulse with 1400 V for 30 ms using the Neon NxT Electroporation System and immediately transferred into cell culture wells containing prewarmed antibiotic-free ImmunoCult XF, IL-2 (1000 IU/ml), AAV6 [35,000 to 45,000 vector genomes (vg) per cell] and HLA-$A2^+$ L cells (without OKT3). Cas9 control T_{reg} cells did not receive any AAV6. T_{reg} cells were maintained in culture for 7 days after electroporation.

On day 12 of culture, edited tCD19$^+$ cells were enriched using the EasySep Human CD19 Positive Selection Kit II (STEMCELL Technologies). All cells were rested overnight by culturing in the presence of IL-2 at 100 IU/ml (T_{reg} cells) or 10 IU/ml (T_{conv} cells), and assays were performed on day 13 of culture.

T_r1 cell isolation, culture, and transduction

T_r1 cells were isolated using an IL-10 capture approach, as previously described (*26*). Briefly, enriched CD4$^+$ T cells were stimulated with Dynabeads Human T-Expander CD3/CD28 (1:16 bead:cell ratio; Thermo Fisher Scientific) overnight, cells primed to secrete IL-10 were stained using the IL-10 Secretion Assay Detection Kit (Miltenyi Biotec), and IL-10$^+$ cells were isolated by cell sorting. Isolated T_r1 cells were stimulated with anti–CD3-loaded L cells, cultured in the presence of IL-2 (100 IU/ml), transduced to express the A2-CAR, restimulated with HLA-A2$^+$ L cells, and rested as described above, in parallel with T_{reg} cells from matched donors.

Flow cytometry and cell sorting

Cells were stained using previously described protocols (*76*) in PBS supplemented with 1% bovine serum and 5 mM EDTA (Sigma-Aldrich). A list of fluorescently conjugated antibodies used is provided in table S1. Dead cells were excluded using Fixable Viability Dye eFluor 780. For samples containing APCs, Fc receptors were blocked by incubating with a polyclonal Fc block for 10 min at room temperature before surface staining. Staining for intracellular markers was performed using the Foxp3/Transcription Factor Staining Buffer Set. Cell proliferation was measured using CPD eFluor 450 or 670 (all from Thermo Fisher Scientific).

Cells were sorted using a MoFlo Astrios (Beckman Coulter) or FACSAria Fusion (BD Biosciences). Flow cytometry data were acquired using an LSRFortessa II, FACSymphony A5, FACSymphony A1 (all from BD Biosciences) or CytoFLEX (Beckman Coulter) and analyzed using FlowJo X (BD Biosciences).

Activation assays and IL-10 secretion analyses

Rested T_{reg} cells were cocultured with blank, HLA-A2$^+$PD-L1$^-$, or HLA-A2$^+$PD-L1$^+$ K562 cells (5:1 T_{reg} cell:K562 ratio) in ImmunoCult XF supplemented with penicillin-streptomycin (100 U/ml) and IL-2 (100 IU/ml). T_r1 cells were similarly treated in cultures supplemented with IL-2 (10 IU/ml). Induced expression of activation markers was determined by flow cytometry after 48 hours. For cytokine secretion analyses, cell culture supernatants were harvested after 72 hours. Alternatively, cytokine secretion kinetics were determined by collecting supernatants every 24 hours; after each collection, cells were washed twice with PBS and re-cultured in fresh medium supplemented with IL-2. Cytokines were measured by LEGENDPlex using a 12-plex Human Th Cytokine Panel (BioLegend).

IL10 qPCR and RNA-seq

For qPCR analyses, T_{reg} cells were stimulated with HLA-A2$^+$ K562 cells. T_{reg} cells were harvested at 24-hour time points following stimulation, washed with PBS, and lysed with Buffer RLT (QIAGEN) supplemented with 1% β-mercaptoethanol (Sigma-Aldrich). RNA was extracted using the RNeasy Micro Kit (QIAGEN) and reverse transcribed using qScript cDNA SuperMix (QuantaBio). qPCRs were performed using PerfeCTa SYBR Green FastMix, Low ROX (QuantaBio), and data were acquired on a ViiA 7 Real-Time PCR System (Applied Biosystems, Thermo Fisher Scientific). Data were analyzed using a $2^{-\Delta\Delta Ct}$ approach with 18*S* and β2-microglobulin as housekeeping controls and the following primers: total *IL10* [forward (FWD), 5′-GCTCAGCACTGCTCTGTTGCCTG-3′; and reverse (REV), 5′-CTCGAAGCATGTTAGGCAGGTTGCC-3′], endogenous *IL10* (FWD, 5′-CAGACTTGCAAAAGAAGGCATGCAC-3′; and REV, 5′-CTCGAAGCATGTTAGGCAGGTTGCC-3′), exogenous *IL10* (FWD, 5′-GTGGAGAAGGCGGCACTCTGGTG-3′; and REV, 5′-CTCGAAGCATGTTAGGCAGGTTGCC-3′), 18*S* (FWD, 5′-CAAGACGGACCAGAGCGAAA-3′; and REV, 5′-GGCGGGTCATGGGAATAAC-3′), and β2-microglobulin (FWD, 5′-ATGTCTCGCTCCGTGGCCTTAG-3′; and REV, 5′-CCATTCTCTGCTGGATGACGTGA-3′).

For RNA-seq, cells were stimulated with HLA-A2 FlowPRA Single Antigen beads (One Lambda) and lysed 16 hours poststimulation using TRIzol, and total RNA was extracted with the PureLink RNA MicroKit (all from Thermo Fisher Scientific). RNA integrity was confirmed to be >8.0 (Agilent 2100 Bioanalyzer or 4200 TapeStation). RNA was prepared using the Illumina Stranded mRNA Prep kit, as per the manufacturer's protocols, and sequencing was performed on the Illumina NextSeq2000 with paired end 59-bp × 59-bp reads. Sequencing data were demultiplexed using llumina's BCL Convert, and de-multiplexed read sequences were then aligned to the *Homo sapiens* (hg38 no Alts, with decoys) reference sequence and the custom exogenous *IL10* sequence using the DRAGEN RNA pipeline. Immunoglobulin gene segments, pseudo genes, sex-linked genes (Y-chromosome and Xist), and genes aligned to virally inserted sequences (CAR, tNGFR, and tCD19) were filtered out as well as genes with <10 counts across samples. Differential expression analysis was performed using DESeq2 in R. Gene annotation was obtained by AnnotationDbi package and visualization with ggplot2, RColorBrewer, pheatmap, and EnhancedVolcano.

CD14$^+$ cell isolation and DC differentiation

CD14$^+$ cells were isolated from PBMCs using the EasySep Human CD14 Positive Selection Kit II (STEMCELL Technologies) to a purity of >97%, as confirmed by flow cytometry. Immature and mDCs were differentiated as previously described (*8*, *77*). Briefly, CD14-enriched cells were resuspended in ImmunoCult XF supplemented with penicillin-streptomycin (100 U/ml) and cultured in the presence of GM-CSF (50 ng/ml) and IL-4 (100 ng/ml; both from STEMCELL Technologies) for 7 days, yielding immature DCs. To mDCs, cultures were additionally supplemented with IL-1β (10 ng/ml) and IL-6 (100 ng/ml; both from STEMCELL Technologies), TNFα (50 ng/ml; eBioscience), and prostaglandin E2 (1 μg/ml; Tocris) from day 5, as well as IFN-γ (50 ng/ml; eBioscience) from day 6.

For assays in which DCs were differentiated in the presence of T_{reg} cells, CD14$^+$ cells from an HLA-A2$^+$ individual were cocultured with T_{reg} cells (10:1 monocyte:T_{reg} cell ratio) in ImmunoCult XF supplemented with penicillin-streptomycin (100 U/ml) and 5% human serum (Wisent Bioproducts) in the presence of GM-CSF (100 ng/ml) and IL-4 (10 ng/ml) for 7 days. Positive control cell cultures (DC10 cells) were additionally supplemented with IL-10 (10 ng/ml; STEMCELL Technologies). The phenotype of the differentiated DCs was then measured by flow cytometry, gating on live CD11c$^+$ cells. In some assays, at the end of the coculture, CD11c$^+$CD4$^-$ DCs were reisolated by cell sorting and stimulated with LPS (200 ng/ml) and IFN-γ (50 ng/ml) for 48 hours, and cell supernatants were collected

to analyze cytokine secretion (*34*). Cytokine secretion was measured using a 10-plex Human M1/M2 Macrophage Panel.

IL-10 functional testing

The immunosuppressive function of IL-10 variants was tested as previously described (*76*). Wild-type and MQIPQ-modified IL-10 protein variants were synthesized by transfecting HEK293T cells with pCCL_wtIL10-tNGFR or pCCL_MQIPQ-IL10-tNGFR (jetPRIME; VWR) and collecting cell culture supernatants after 24 hours. Control cells were mock transfected. Secreted IL-10 was quantified by LEGENDPlex using a 10-plex Human M1/M2 Macrophage Panel.

To test the function of the IL-10 variants, freshly isolated $CD14^+$ cells were cultured overnight in ImmunoCult XF supplemented with penicillin-streptomycin (100 U/ml) and wild-type IL-10 or MQIPQ-modified IL-10 (5 μg/ml). The following day, monocytes were stimulated with LPS (200 ng/ml) and 5 mM adenosine 5′-triphosphate (both from InvivoGen). Monocyte supernatants were collected 5 hours post-stimulation, and cytokine production was measured by LEGENDPlex using a 10-plex Human M1/M2 Macrophage Panel.

Suppression assays

All suppression assays were performed in ImmunoCult XF supplemented with penicillin-streptomycin (100 U/ml) and 5% human serum. For DC suppression assays, T_{reg} cells were cocultured with mature $HLA\text{-}A2^+$ DCs in the presence of IL-2 (100 IU/ml) for 3 days (with no additional exogenous cytokines) after which the DC phenotype was measured by flow cytometry.

For polyclonal suppression assays, T_{reg} cells were labeled with CPD-eFluor 670 (Thermo Fisher Scientific), serially diluted and cocultured with allogeneic $HLA\text{-}A2^-$ PBMCs that were labeled with CPD-eFluor 450, and activated with Dynabeads Human T-Expander CD3/CD28 (1:8 bead:PBMC ratio; Thermo Fisher Scientific). Cells were stained and analyzed by flow cytometry after 4 days of culture. Responder T cell division was measured using division indices and used to calculate % suppression (inverse of percent responder T cell proliferation) relative to responder T cells cultured alone. Suppression of CD80 and CD86 expression on $CD19^+CD4^-$ B cells in the responder PBMC population was concurrently measured and is reported relative to responders cultured alone.

For antigen-specific alloantigen-dependent suppression assays, $HLA\text{-}A3^-$ T_{reg} cells were labeled with CPD eFluor 670, serially diluted, and cocultured with allogeneic $HLA\text{-}A2^+$ mDCs. After 3 days, $CD3^+$ responder T cells (previously enriched from an $HLA\text{-}A3^+$ individual using the EasySep Human CD3 Positive Selection Kit II; STEMCELL Technologies) were labeled with CPD eFluor 450 and added to the cocultures at a 5:1 responder T cell:DC ratio. Cocultures were maintained for a further 4 days before being stained and analyzed by flow cytometry. % Suppression was calculated as described above, gating on $CD4^+HLA\text{-}A3^+$CPD eFluor 670^- responder cells.

Antigen-specific GAD65 peptide-dependent suppression assays were performed using frozen $CD4^+$ responder T cells that expressed the 4.13-TCR (*29*). To generate these responder T cells, enriched $CD4^+$ T cells (EasySep Human CD4 Positive Selection Kit II, STEMCELL Technologies) were stimulated with Dynabeads Human T-Expander CD3/CD28 (3:1 bead:T cell ratio), lentivirally transduced to express the 4.13-TCR, tNGFR-enriched (Human CD271 MicroBeads Kit, Miltenyi Biotec), and frozen on day 9 of culture (*78*). For suppression assays, T_{reg} cells were serially diluted and cocultured with $HLA\text{-}A2^+HLA\text{-}DR4^+$ immature DCs. After 1 to 2 days, 4.13-TCR^+ T cells were thawed and added to the cocultures at a 5:1 responder T cell:DC ratio along with 1 nM GAD65 peptide (NFIRMVISNPAAT). In some experiments, control DCs were pulsed with an irrelevant hemagglutinin peptide (PKYVKQNTLKLAT). Cocultures were maintained for a further 2 days before being stained and analyzed by flow cytometry. % Suppression was determined by measuring inhibition of Ki67 expression in the $CD4^+$mTCRβ$^+$CPD eFluor 670^- responder T cells.

In vivo A2-CAR T_{reg} cell chronic stimulation model

To chronically stimulate A2-CAR T_{reg} cells in vivo, A2-NSG mice (8 to 17 weeks old) were preconditioned by sublethal irradiation (150 cGy) 1 day before starting the experiment or treated with two doses of busulfan (15 mg/kg per dose) 24 and 48 hours before starting the experiment. Mice were then intravenously (tail vein) administered 1.5×10^6 to 3.2×10^6 T_{reg} cells with an equal number of autologous $HLA\text{-}A2^-$ PBMCs as an in vivo source of IL-2. Control mice were administered saline or PBMCs alone. Mice were routinely monitored with no evidence of xenoGVHD development and humanely euthanized 21 days post-infusion. Cardiac blood was collected, and red blood cells were lysed with ammonium chloride (STEMCELL Technologies). Spleens were dissociated through 70-μm cell strainers to obtain single-cell suspensions. Resulting lymphocytes were stained and analyzed by flow cytometry or cell sorted for TSDR analysis.

In vivo graft-versus-host-disease model

NSG mice (14 to 18 weeks old) were preconditioned with two doses of busulfan (15 mg/kg per dose) 24 and 48 hours before starting the experiment. Mice were then intravenously (tail vein) administered 4×10^6 $HLA\text{-}A2^{pos}CD4^+$ T_{conv} cells without or with allogeneic A2-CAR T_{reg} cells at the stated ratios. Control mice were administered T_{conv} cells alone. Mice were routinely monitored for signs of xenoGVHD (scoring based on weight, activity, posture, fur texture, skin integrity, signs of pain, stool consistency, dehydration, and rectal bleeding) (*79*) and humanely euthanized at 7 or 10 weeks post-infusion or when predefined end point criteria were met. Human cell engraftment was tracked by weekly bleeding from the saphenous vein.

Upon euthanasia, lymphocytes from the blood and spleen were isolated as detailed above. Intestinal tissue from the duodenum, jejunum, ileum, and colon was digested with collagenase VIII (Sigma-Aldrich), and lamina propria lymphocytes were acquired using Percoll density centrifugation (GE Healthcare), as previously described (*78*, *80*). Ear skin was mechanically and enzymatically digested with collagenase XI and hyaluronidase (both from Sigma-Aldrich), and cells were passed through 70-μm cell strainers to obtain single-cell suspensions. Resulting cell preparations were stained and analyzed by flow cytometry. Absolute cell numbers were calculated by adding 123count eBeads (Thermo Fisher Scientific) to each sample before acquisition.

TSDR analysis

DNA was isolated and bisulfite converted using the EZ Direct Kit (Zymo Research). The TSDR was PCR amplified using the AllTaq PCR Core Kit (QIAGEN) and the following primers: FWD, AGAA-ATTTGTGGGGTGGGGTAT); and REV (biotinylated), AT-CTAC-ATCTAAACCCTATTATCACAACC. PCR products were run on a

Q96 MD pyrosequencing system (QIAGEN) using the following sequencing primer: AGAAATTTGTGGGGTGGG. Data were analyzed using Pyro Q-CpG software (Biotage) by comparing cytosine versus thymine incorporation at 7-CpG sites in the TSDR.

Statistical analysis

Flow cytometry data were analyzed using FlowJo X, LLC (BD Biosciences). Data were analyzed using GraphPad Prism 10 (La Jolla) and presented as means ± SEM with the contribution of each donor shown. Statistical significance was determined using paired two-tailed Student's *t* tests, repeated measures mixed-effects analyses with Fisher's least significant difference multiple comparisons, one-way/two-way analysis of variance (ANOVA), or log-rank Mantel-Cox tests. For RNA-seq analyses, Wald tests with Benjamini-Hochberg correction were used. *P* values are provided throughout where $P < 0.05$ was considered significant.

Supplementary Materials

This PDF file includes:

Figs. S1 to S9

Table S1

REFERENCES AND NOTES

1. C. M. Wardell, D. A. Boardman, M. K. Levings, Harnessing the biology of regulatory T cells to treat disease. *Nat. Rev. Drug Discov.* **24**, 93–111 (2024).
2. J. A. Bluestone, J. H. Buckner, M. Fitch, S. E. Gitelman, S. Gupta, M. K. Hellerstein, K. C. Herold, A. Lares, M. R. Lee, K. Li, W. Liu, S. A. Long, L. M. Masiello, V. Nguyen, A. L. Putnam, M. Rieck, P. H. Sayre, Q. Tang, Type 1 diabetes immunotherapy using polyclonal regulatory T cells. *Sci. Transl. Med.* **7**, 315ra189 (2015).
3. B. Sawitzki, P. N. Harden, P. Reinke, A. Moreau, J. A. Hutchinson, D. S. Game, Q. Tang, E. C. Guinan, M. Battaglia, W. J. Burlingham, I. S. D. Roberts, M. Streitz, R. Josien, C. A. Böger, C. Scottà, J. F. Markmann, J. L. Hester, K. Juerchott, C. Braudeau, B. James, L. Contreras-Ruiz, J. B. van der Net, T. Bergler, R. Caldara, W. Petchey, M. Edinger, N. Dupas, M. Kapinsky, I. Mutzbauer, N. M. Otto, R. Öllinger, M. P. Hernandez-Fuentes, F. Issa, N. Ahrens, C. Meyenberg, S. Karitzky, U. Kunzendorf, S. J. Knechtle, J. Grinyó, P. J. Morris, L. Brent, A. Bushell, L. A. Turka, J. A. Bluestone, R. I. Lechler, H. J. Schlitt, M. C. Cuturi, S. Schlickeiser, P. J. Friend, T. Miloud, A. Scheffold, A. Secchi, K. Crisalli, S.-M. Kang, R. Hilton, B. Banas, G. Blancho, H.-D. Volk, G. Lombardi, K. J. Wood, E. K. Geissler, Regulatory cell therapy in kidney transplantation (The ONE Study): A harmonised design and analysis of seven non-randomised, single-arm, phase 1/2A trials. *Lancet* **395**, 1627–1639 (2020).
4. D. Boardman, J. Maher, R. Lechler, L. Smyth, G. Lombardi, Antigen-specificity using chimeric antigen receptors: The future of regulatory T-cell therapy? *Biochem. Soc. Trans.* **44**, 342–348 (2016).
5. K. G. MacDonald, R. E. Hoeppli, Q. Huang, J. Gillies, D. S. Luciani, P. C. Orban, R. Broady, M. K. Levings, Alloantigen-specific regulatory T cells generated with a chimeric antigen receptor. *J. Clin. Invest.* **126**, 1413–1424 (2016).
6. D. A. Boardman, C. Philippeos, G. O. Fruhwirth, M. A. Ibrahim, R. F. Hannen, D. Cooper, F. M. Marelli-Berg, F. M. Watt, R. I. Lechler, J. Maher, L. A. Smyth, G. Lombardi, Expression of a chimeric antigen receptor specific for donor HLA class I enhances the potency of human regulatory T cells in preventing human skin transplant rejection. *Am. J. Transplant.* **17**, 931–943 (2017).
7. N. A. Dawson, C. Lamarche, R. E. Hoeppli, P. Bergqvist, V. C. Fung, E. M. Iver, Q. Huang, J. Gillies, M. Speck, P. C. Orban, J. W. Bush, M. Mojibian, M. K. Levings, Systematic testing and specificity mapping of alloantigen-specific chimeric antigen receptors in regulatory T cells. *JCI Insight* **4**, e123672 (2019).
8. N. A. J. Dawson, I. Rosado-Sánchez, G. E. Novakovsky, V. C. W. Fung, Q. Huang, E. M. Iver, G. Sun, J. Gillies, M. Speck, P. C. Orban, M. Mojibian, M. K. Levings, Functional effects of chimeric antigen receptor co-receptor signaling domains in human regulatory T cells. *Sci. Transl. Med.* **12**, eaaz3866 (2020).
9. A. Sicard, C. Lamarche, M. Speck, M. Wong, I. Rosado- Sánchez, M. Blois, N. Glaichenhaus, M. Mojibian, M. K. Levings, Donor-specific chimeric antigen receptor Tregs limit rejection in naive but not sensitized allograft recipients. *Am. J. Transplant.* **20**, 1562–1573 (2020).
10. J. C. Wagner, E. Ronin, P. Ho, Y. Peng, Q. Tang, Anti-HLA-A2-CAR Tregs prolong vascularized mouse heterotopic heart allograft survival. *Am. J. Transplant.* **22**, 2237–2245 (2022).
11. S. Simon, N. Labarriere, PD-1 expression on tumor-specific T cells: Friend or foe for immunotherapy? *Oncoimmunology* **7**, e1364828 (2017).
12. E. A. Stadtmauer, J. A. Fraietta, M. M. Davis, A. D. Cohen, K. L. Weber, E. Lancaster, P. A. Mangan, I. Kulikovskaya, M. Gupta, F. Chen, L. Tian, V. E. Gonzalez, J. Xu, I.-Y. Jung, J. J. Melenhorst, G. Plesa, J. Shea, T. Matlawski, A. Cervini, A. L. Gaymon, S. Desjardins, A. Lamontagne, J. Salas-Mckee, A. Fesnak, D. L. Siegel, B. L. Levine, J. K. Jadlowsky, R. M. Young, A. Chew, W.-T. Hwang, E. O. Hexner, B. M. Carreno, C. L. Nobles, F. D. Bushman, K. R. Parker, Y. Qi, A. T. Satpathy, H. Y. Chang, Y. Zhao, S. F. Lacey, C. H. June, CRISPR-engineered T cells in patients with refractory cancer. *Science* **367**, eaba7365 (2020).
13. Y. Lu, J. Xue, T. Deng, X. Zhou, K. Yu, L. Deng, M. Huang, X. Yi, M. Liang, Y. Wang, H. Shen, R. Tong, W. Wang, L. Li, J. Song, J. Li, X. Su, Z. Ding, Y. Gong, J. Zhu, Y. Wang, B. Zou, Y. Zhang, Y. Li, L. Zhou, Y. Liu, M. Yu, Y. Wang, X. Zhang, L. Yin, X. Xia, Y. Zeng, Q. Zhou, B. Ying, C. Chen, Y. Wei, W. Li, T. Mok, Safety and feasibility of CRISPR-edited T cells in patients with refractory non-small-cell lung cancer. *Nat. Med.* **26**, 732–740 (2020).
14. Z. Wang, N. Li, K. Feng, M. Chen, Y. Zhang, Y. Liu, Q. Yang, J. Nie, N. Tang, X. Zhang, C. Cheng, L. Shen, J. He, X. Ye, W. Cao, H. Wang, W. Han, Phase I study of CAR-T cells with PD-1 and TCR disruption in mesothelin-positive solid tumors. *Cell. Mol. Immunol.* **18**, 2188–2198 (2021).
15. Y. Hu, C. Zu, M. Zhang, G. Wei, W. Li, S. Fu, R. Hong, L. Zhou, W. Wu, J. Cui, D. Wang, B. Du, M. Liu, J. Zhang, H. Huang, Safety and efficacy of CRISPR-based non-viral PD1 locus specifically integrated anti-CD19 CAR-T cells in patients with relapsed or refractory non-Hodgkin's lymphoma: A first-in-human phase I study. *EClinicalMedicine* **60**, 102010 (2023).
16. D. E. Lowther, B. A. Goods, L. E. Lucca, B. A. Lerner, K. Raddassi, D. van Dijk, A. L. Hernandez, X. Duan, M. Gunel, V. Coric, S. Krishnaswamy, J. C. Love, D. A. Hafler, PD-1 marks dysfunctional regulatory T cells in malignant gliomas. *JCI Insight* **1**, e85935 (2016).
17. J. Xiao, L. Zhang, Y. Dong, X. Liu, L. Peng, Y. Yang, Y. Wang, PD-1 upregulation is associated with exhaustion of regulatory T cells and reflects immune activation in HIV-1-infected individuals. *AIDS Res. Hum. Retroviruses* **35**, 444–452 (2019).
18. M. Sambucci, F. Gargano, V. De Rosa, M. De Bardi, M. Picozza, R. Placido, S. Ruggieri, A. Capone, C. Gasperini, G. Matarese, L. Battistini, G. Borsellino, FoxP3 isoforms and PD-1 expression by T regulatory cells in multiple sclerosis. *Sci. Rep.* **8**, 3674 (2018).
19. T. Kamada, Y. Togashi, C. Tay, D. Ha, A. Sasaki, Y. Nakamura, E. Sato, S. Fukuoka, Y. Tada, A. Tanaka, H. Morikawa, A. Kawazoe, T. Kinoshita, K. Shitara, S. Sakaguchi, H. Nishikawa, PD-1^{+} regulatory T cells amplified by PD-1 blockade promote hyperprogression of cancer. *Proc. Natl. Acad. Sci. U.S.A.* **116**, 9999–10008 (2019).
20. S. Kumagai, Y. Togashi, T. Kamada, E. Sugiyama, H. Nishinakamura, Y. Takeuchi, K. Vitaly, K. Itahashi, Y. Maeda, S. Matsui, T. Shibahara, Y. Yamashita, T. Irie, A. Tsuge, S. Fukuoka, A. Kawazoe, H. Udagawa, K. Kirita, K. Aokage, G. Ishii, T. Kuwata, K. Nakama, M. Kawazu, T. Ueno, N. Yamazaki, K. Goto, M. Tsuboi, H. Mano, T. Doi, K. Shitara, H. Nishikawa, The PD-1 expression balance between effector and regulatory T cells predicts the clinical efficacy of PD-1 blockade therapies. *Nat. Immunol.* **21**, 1346–1358 (2020).
21. J. A. Perry, L. Shallberg, J. T. Clark, J. A. Gullicksrud, J. H. De Long, B. B. Douglas, A. P. Hart, Z. Lanzar, K. O'Dea, C. Konradt, J. Park, J. R. Kuchroo, D. Grubaugh, A. G. Zaretsky, I. E. Brodsky, R. de Waal Malefyt, D. A. Christian, A. H. Sharpe, C. A. Hunter, PD-L1–PD-1 interactions limit effector regulatory T cell populations at homeostasis and during infection. *Nat. Immunol.* **23**, 743–756 (2022).
22. M. Wong, A. La Cava, B. H. Hahn, Blockade of programmed death-1 in young (New Zealand Black x New Zealand White)F_1 mice promotes the suppressive capacity of CD4^{+} regulatory T cells protecting from lupus-like disease. *J. Immunol.* **190**, 5402–5410 (2013).
23. C. L. Tan, J. R. Kuchroo, P. T. Sage, D. Liang, L. M. Francisco, J. Buck, Y. R. Thaker, Q. Zhang, S. L. McArdel, V. R. Juneja, S. J. Lee, S. B. Lovitch, C. Lian, G. F. Murphy, B. R. Blazar, D. A. A. Vignali, G. J. Freeman, A. H. Sharpe, PD-1 restraint of regulatory T cell suppressive activity is critical for immune tolerance. *J. Exp. Med.* **218**, e20182232 (2021).
24. M. K. Levings, R. Sangregorio, C. Sartirana, A. L. Moschin, M. Battaglia, P. C. Orban, M. G. Roncarolo, Human CD25^{+}CD4^{+} T suppressor cell clones produce transforming growth factor β, but not interleukin 10, and are distinct from type 1 T regulatory cells. *J. Exp. Med.* **196**, 1335–1346 (2002).
25. Y. Yao, J. Vent-Schmidt, M. D. McGeough, M. Wong, H. M. Hoffman, T. S. Steiner, M. K. Levings, Tr1 cells, but not Foxp3^{+} regulatory T cells, suppress NLRP3 inflammasome activation via an IL-10–dependent mechanism. *J. Immunol.* **195**, 488–497 (2015).
26. L. Cook, M. Stahl, X. Han, A. Nazli, K. N. MacDonald, M. Q. Wong, K. Tsai, S. Dizzell, K. Jacobson, B. Bressler, C. Kaushic, B. A. Vallance, T. S. Steiner, M. K. Levings, Suppressive and gut-reparative functions of human Type 1 T regulatory cells. *Gastroenterology* **157**, 1584–1598 (2019).
27. M. G. Roncarolo, S. Gregori, R. Bacchetta, M. Battaglia, N. Gagliani, The biology of T regulatory Type 1 cells and their therapeutic application in immune-mediated diseases. *Immunity* **49**, 1004–1019 (2018).
28. M. Saraiva, P. Vieira, A. O'Garra, Biology and therapeutic potential of interleukin-10. *J. Exp. Med.* **217**, e20190418 (2020).
29. W. I. Yeh, H. R. Seay, B. Newby, A. L. Posgai, F. B. Moniz, A. Michels, C. E. Mathews, J. A. Bluestone, T. M. Brusko, Avidity and bystander suppressive capacity of human

regulatory T cells expressing de novo autoreactive T-cell receptors in type 1 diabetes. *Front. Immunol.* **8**, 1313 (2017).
30. P. T. Walsh, D. K. Taylor, L. A. Turka, Tregs and transplantation tolerance. *J. Clin. Invest.* **114**, 1398–1403 (2004).
31. A. H. Sharpe, K. E. Pauken, The diverse functions of the PD1 inhibitory pathway. *Nat. Rev. Immunol.* **18**, 153–167 (2018).
32. Y. R. Mohseni, A. Saleem, S. L. Tung, C. Dudreuilh, C. Lang, Q. Peng, A. Volpe, G. Adigbli, A. Cross, J. Hester, F. Farzaneh, C. Scotta, R. I. Lechler, F. Issa, G. O. Fruhwirth, G. Lombardi, Chimeric antigen receptor-modified human regulatory T cells that constitutively express IL-10 maintain their phenotype and are potently suppressive. *Eur. J. Immunol.* **51**, 2522–2530 (2021).
33. S. Gregori, D. Tomasoni, V. Pacciani, M. Scirpoli, M. Battaglia, C. F. Magnani, E. Hauben, M. G. Roncarolo, Differentiation of type 1 T regulatory cells (Tr1) by tolerogenic DC-10 requires the IL-10-dependent ILT4/HLA-G pathway. *Blood* **116**, 935–944 (2010).
34. L. Passeri, G. Andolfi, V. Bassi, F. Russo, G. Giacomini, C. Laudisa, I. Marrocco, L. Cesana, M. Di Stefano, L. Fanti, P. Sgaramella, S. Vitale, C. Ziparo, R. Auricchio, G. Barera, G. Di Nardo, R. Troncone, C. Gianfrani, A. Annoni, L. Passerini, S. Gregori, Tolerogenic IL-10-engineered dendritic cell-based therapy to restore antigen-specific tolerance in T cell mediated diseases. *J. Autoimmun.* **138**, 103051 (2023).
35. A. M. Shiri, T. Zhang, T. Bedke, D. E. Zazara, L. Zhao, J. Lücke, M. Sabihi, A. Fazio, S. Zhang, D. V. F. Tauriello, E. Batlle, B. Steglich, J. Kempski, T. Agalioti, M. Nawrocki, Y. Xu, K. Riecken, I. Liebold, L. Brockmann, L. Konczalla, L. Bosurgi, B. Mercanoglu, P. Seeger, N. Küsters, P. M. Lykoudis, A. Heumann, P. C. Arck, B. Fehse, P. Busch, R. Grotelüschen, O. Mann, J. R. Izbicki, T. Hackert, R. A. Flavell, N. Gagliani, A. D. Giannou, S. Huber, IL-10 dampens antitumor immunity and promotes liver metastasis via PD-L1 induction. *J. Hepatol.* **80**, 634–644 (2024).
36. A. M. Pesenacker, V. Chen, J. Gillies, C. Speake, A. K. Marwaha, A. Sun, S. Chow, R. Tan, T. Elliott, J. P. Dutz, S. J. Tebbutt, M. K. Levings, Treg gene signatures predict and measure type 1 diabetes trajectory. *JCI Insight* **4**, e123879 (2019).
37. A. Joss, M. Akdis, A. Faith, K. Blaser, C. A. Akdis, IL-10 directly acts on T cells by specifically altering the CD28 co-stimulation pathway. *Eur. J. Immunol.* **30**, 1683–1690 (2000).
38. C. A. Akdis, A. Joss, M. Akdis, A. Faith, K. Blaser, A molecular basis for T cell suppression by IL-10: CD28-associated IL-10 receptor inhibits CD28 tyrosine phosphorylation and phosphatidylinositol 3-kinase binding. *FASEB J.* **14**, 1666–1668 (2000).
39. M. Kamanaka, S. Huber, L. A. Zenewicz, N. Gagliani, C. Rathinam, W. O'Connor Jr., Y. Y. Wan, S. Nakae, Y. Iwakura, L. Hao, R. A. Flavell, Memory/effector (CD45RB^{lo}) CD4 T cells are controlled directly by IL-10 and cause IL-22–dependent intestinal pathology. *J. Exp. Med.* **208**, 1027–1040 (2011).
40. X. Rui, F. A. Calderon, H. Wobma, U. Gerdemann, A. Albanese, L. Cagnin, C. M. Guckin, K. A. Michaelis, K. Naqvi, B. R. Blazar, V. Tkachev, L. S. Kean, Human OX40L-CAR-T$_{regs}$ target activated antigen-presenting cells and control T cell alloreactivity. *Sci. Transl. Med.* **16**, eadj9331 (2024).
41. K. Ou, D. Hamo, A. Schulze, A. Roemhild, D. Kaiser, G. Gasparoni, A. Salhab, G. Zarrinrad, L. Amini, S. Schlickeiser, M. Streitz, J. Walter, H. D. Volk, M. Schmueck-Henneresse, P. Reinke, J. K. Polansky, Strong expansion of human regulatory T cells for adoptive cell therapy results in epigenetic changes which may impact their survival and function. *Front. Cell Dev. Biol.* **9**, 751590 (2021).
42. C. G. Feng, M. C. Kullberg, D. Jankovic, A. W. Cheever, P. Caspar, R. L. Coffman, A. Sher, Transgenic mice expressing human interleukin-10 in the antigen-presenting cell compartment show increased susceptibility to infection with Mycobacterium avium associated with decreased macrophage effector function and apoptosis. *Infect. Immun.* **70**, 6672–6679 (2002).
43. Y. Song, N. Wang, L. Chen, L. Fang, Tr1 cells as a key regulator for maintaining immune homeostasis in transplantation. *Front. Immunol.* **12**, 671579 (2021).
44. E. Gianchecchi, A. Fierabracci, Inhibitory receptors and pathways of lymphocytes: The role of PD-1 in Treg development and their involvement in autoimmunity onset and cancer progression. *Front. Immunol.* **9**, 2374 (2018).
45. J. Cai, D. Wang, G. Zhang, X. Guo, The role of PD-1/PD-L1 axis in Treg development and function: Implications for cancer immunotherapy. *Onco. Targets. Ther.* **12**, 8437–8445 (2019).
46. L. M. Francisco, V. H. Salinas, K. E. Brown, V. K. Vanguri, G. J. Freeman, V. K. Kuchroo, A. H. Sharpe, PD-L1 regulates the development, maintenance, and function of induced regulatory T cells. *J. Exp. Med.* **206**, 3015–3029 (2009).
47. S. Amarnath, C. W. Mangus, J. C. M. Wang, F. Wei, A. He, V. Kapoor, J. E. Foley, P. R. Massey, T. C. Felizardo, J. L. Riley, B. L. Levine, C. H. June, J. A. Medin, D. H. Fowler, The PDL1-PD1 axis converts human TH1 cells into regulatory T cells. *Sci. Transl. Med.* **3**, 111ra120 (2011).
48. E. McGowan, Q. Lin, G. Ma, H. Yin, S. Chen, Y. Lin, PD-1 disrupted CAR-T cells in the treatment of solid tumors: Promises and challenges. *Biomed. Pharmacother.* **121**, 109625 (2020).
49. L. J. Rupp, K. Schumann, K. T. Roybal, R. E. Gate, C. J. Ye, W. A. Lim, A. Marson, CRISPR/Cas9-mediated PD-1 disruption enhances anti-tumor efficacy of human chimeric antigen receptor T cells. *Sci. Rep.* **7**, 737 (2017).
50. J. Zhang, Y. Hu, J. Yang, W. Li, M. Zhang, Q. Wang, L. Zhang, G. Wei, Y. Tian, K. Zhao, A. Chen, B. Tan, J. Cui, D. Li, Y. Li, Y. Qi, D. Wang, Y. Wu, D. Li, B. Du, M. Liu, H. Huang, Non-viral, specifically targeted CAR-T cells achieve high safety and efficacy in B-NHL. *Nature* **609**, 369–374 (2022).
51. S. Kim, C. I. Park, S. Lee, H. R. Choi, C. H. Kim, Reprogramming of IL-12 secretion in the PDCD1 locus improves the anti-tumor activity of NY-ESO-1 TCR-T cells. *Front. Immunol.* **14**, 1062365 (2023).
52. M. S. Simic, P. B. Watchmaker, S. Gupta, Y. Wang, S. A. Sagan, J. Duecker, C. Shepherd, D. Diebold, P. Pineo-Cavanaugh, J. Haegelin, R. Zhu, B. Ng, W. Yu, Y. Tonai, L. Cardarelli, N. R. Reddy, S. S. Sidhu, O. Troyanskaya, S. L. Hauser, M. R. Wilson, S. S. Zamvil, H. Okada, W. A. Lim, Programming tissue-sensing T cells that deliver therapies to the brain. *Science* **386**, (2024).
53. X. Wang, K. Wong, W. Ouyang, S. Rutz, Targeting IL-10 family cytokines for the treatment of human diseases. *Cold Spring Harb. Perspect. Biol.* **11**, a028548 (2019).
54. A. Saxena, S. Khosraviani, S. Noel, D. Mohan, T. Donner, A. R. Hamad, Interleukin-10 paradox: A potent immunoregulatory cytokine that has been difficult to harness for immunotherapy. *Cytokine* **74**, 27–34 (2015).
55. R. D. Huhn, E. Radwanski, J. Gallo, M. B. Affrime, R. Sabo, G. Gonyo, A. Monge, D. L. Cutler, Pharmacodynamics of subcutaneous recombinant human interleukin-10 in healthy volunteers. *Clin. Pharmacol. Ther.* **62**, 171–180 (1997).
56. J. Rana, D. J. Perry, S. R. P. Kumar, M. Munoz-Melero, R. Saboungi, T. M. Brusko, M. Biswas, CAR- and TRuC-redirected regulatory T cells differ in capacity to control adaptive immunity to FVIII. *Mol. Ther.* **29**, 2660–2676 (2021).
57. Y. Zhao, J. Chen, M. Andreatta, B. Feng, Y. Q. Xie, M. Wenes, Y. Wang, M. Gao, X. Hu, P. Romero, S. Carmona, J. Sun, Y. Guo, L. Tang, IL-10-expressing CAR T cells resist dysfunction and mediate durable clearance of solid tumors and metastases. *Nat. Biotechnol.* **42**, 1693–1704 (2024).
58. K. W. Moore, R. de Waal Malefyt, R. L. Coffman, A. O'Garra, Interleukin-10 and the interleukin-10 receptor. *Annu. Rev. Immunol.* **19**, 683–765 (2001).
59. N. Yogev, T. Bedke, Y. Kobayashi, L. Brockmann, D. Lukas, T. Regen, A. L. Croxford, A. Nikolav, N. Hovelmeyer, E. von Stebut, M. Prinz, C. Ubeda, K. J. Maloy, N. Gagliani, R. A. Flavell, A. Waisman, S. Huber, CD4$^+$ T-cell-derived IL-10 promotes CNS inflammation in mice by sustaining effector T cell survival. *Cell Rep.* **38**, 110565 (2022).
60. X. Liu, R. Alli, M. Steeves, P. Nguyen, P. Vogel, T. L. Geiger, The T cell response to IL-10 alters cellular dynamics and paradoxically promotes central nervous system autoimmunity. *J. Immunol.* **189**, 669–678 (2012).
61. H. Groux, M. Bigler, J. E. de Vries, M. G. Roncarolo, Inhibitory and stimulatory effects of IL-10 on human CD8+ T cells. *J. Immunol.* **160**, 3188–3193 (1998).
62. C. Gorby, J. Sotolongo Bellon, S. Wilmes, W. Warda, E. Pohler, P. K. Fyfe, A. Cozzani, C. Ferrand, M. R. Walter, S. Mitra, J. Piehler, I. Moraga, Engineered IL-10 variants elicit potent immunomodulatory effects at low ligand doses. *Sci. Signal.* **13**, eabc0653 (2020).
63. F. Minshawi, S. Lanvermann, E. McKenzie, R. Jeffery, K. Couper, S. Papoutsopoulou, A. Roers, W. Muller, The generation of an engineered interleukin-10 protein with improved stability and biological function. *Front. Immunol.* **11**, 1794 (2020).
64. M. H. Butt, M. Zaman, A. Ahmad, R. Khan, T. H. Mallhi, M. M. Hasan, Y. H. Khan, S. Hafeez, E. E. S. Massoud, M. H. Rahman, S. Cavalu, Appraisal for the potential of viral and nonviral vectors in gene therapy: A review. *Genes* **13**, 1370 (2022).
65. T. Y. Yang, M. Braun, W. Lembke, F. McBlane, J. Kamerud, S. DeWall, E. Tarcsa, X. Fang, L. Hofer, U. Kavita, V. V. Upreti, S. Gupta, L. Loo, A. J. Johnson, R. K. Chandode, K. G. Stubenrauch, M. Vinzing, C. Q. Xia, V. Jawa, Immunogenicity assessment of AAV-based gene therapies: An IQ consortium industry white paper. *Mol Ther Methods Clin Dev* **26**, 471–494 (2022).
66. Y. P. Rubtsov, J. P. Rasmussen, E. Y. Chi, J. Fontenot, L. Castelli, X. Ye, P. Treuting, L. Siewe, A. Roers, W. R. Henderson Jr., W. Muller, A. Y. Rudensky, Regulatory T cell-derived interleukin-10 limits inflammation at environmental interfaces. *Immunity* **28**, 546–558 (2008).
67. A. J. Lam, D. T. S. Lin, J. K. Gillies, P. Uday, A. M. Pesenacker, M. S. Kobor, M. K. Levings, Optimized CRISPR-mediated gene knockin reveals FOXP3-independent maintenance of human Treg identity. *Cell Rep.* **36**, 109494 (2021).
68. R. de Waal Malefyt, S. Verma, M. T. Bejarano, M. Ranes-Goldberg, M. Hill, H. Spits, CD2/LFA-3 or LFA-1/ICAM-1 but not CD28/B7 interactions can augment cytotoxicity by virus-specific CD8$^+$ cytotoxic T lymphocytes. *Eur. J. Immunol.* **23**, 418–424 (1993).
69. X. Liu, Y. Zhang, C. Cheng, A. W. Cheng, X. Zhang, N. Li, C. Xia, X. Wei, X. Liu, H. Wang, CRISPR-Cas9-mediated multiplex gene editing in CAR-T cells. *Cell Res.* **27**, 154–157 (2017).
70. X. Guo, H. Jiang, B. Shi, M. Zhou, H. Zhang, Z. Shi, G. Du, H. Luo, X. Wu, Y. Wang, R. Sun, Z. Li, Disruption of PD-1 enhanced the anti-tumor activity of chimeric antigen receptor T cells against hepatocellular carcinoma. *Front. Pharmacol.* **9**, 1118 (2018).
71. T. Nakazawa, A. Natsume, F. Nishimura, T. Morimoto, R. Matsuda, M. Nakamura, S. Yamada, I. Nakagawa, Y. Motoyama, Y. S. Park, T. Tsujimura, T. Wakabayashi, H. Nakase, Effect of CRISPR/Cas9-mediated PD-1-disrupted primary human third-generation CAR-T cells targeting EGFRvIII on in vitro human glioblastoma cell growth. *Cells* **9**, 998 (2020).
72. J. Ren, X. Liu, C. Fang, S. Jiang, C. H. June, Y. Zhao, Multiplex genome editing to generate universal CAR T cells resistant to PD1 inhibition. *Clin. Cancer Res.* **23**, 2255–2266 (2017).

73. K. Schumann, S. Lin, E. Boyer, D. R. Simeonov, M. Subramaniam, R. E. Gate, G. E. Haliburton, C. J. Ye, J. A. Bluestone, J. A. Doudna, A. Marson, Generation of knock-in primary human T cells using Cas9 ribonucleoproteins. *Proc. Natl. Acad. Sci. U.S.A.* **112**, 10437–10442 (2015).
74. W. Hu, Z. Zi, Y. Jin, G. Li, K. Shao, Q. Cai, X. Ma, F. Wei, CRISPR/Cas9-mediated PD-1 disruption enhances human mesothelin-targeted CAR T cell effector functions. *Cancer Immunol. Immunother.* **68**, 365–377 (2019).
75. L. Marotte, S. Simon, V. Vignard, E. Dupre, M. Gantier, J. Cruard, J. B. Alberge, M. Hussong, C. Deleine, J. M. Heslan, J. Shaffer, T. Beauvais, J. Gaschet, E. Scotet, D. Fradin, A. Jarry, T. Nguyen, N. Labarriere, Increased antitumor efficacy of PD-1-deficient melanoma-specific human lymphocytes. *J. Immunother. Cancer* **8**, e000311 (2020).
76. D. A. Boardman, R. V. Garcia, S. M. Ivison, B. Bressler, T. M. Dhar, Q. Zhao, M. K. Levings, Pharmacological inhibition of RORC2 enhances human Th17-Treg stability and function. *Eur. J. Immunol.* **50**, 1400–1411 (2020).
77. Q. Huang, A. J. Lam, D. A. Boardman, N. A. J. Dawson, M. K. Levings, Suppression of human dendritic cells by regulatory T cells. *Bio. Protoc.* **11**, e4217 (2021).
78. D. A. Boardman, M. Q. Wong, W. D. Rees, D. Wu, M. E. Himmel, P. C. Orban, J. Vent-Schmidt, N. C. Zachos, T. S. Steiner, M. K. Levings, Flagellin-specific human CAR Tregs for immune regulation in IBD. *J. Autoimmun.* **134**, 102961 (2023).
79. M. Haque, D. A. Boardman, A. J. Lam, K. N. MacDonald, L. Sanderink, Q. Huang, V. C. W. Fung, S. Ivison, M. Mojibian, M. K. Levings, Modelling graft-versus-host disease in mice using human peripheral blood mononuclear cells. *Bio. Protoc.* **12**, e4566 (2022).
80. D. Wu, M. Q. Wong, J. Vent-Schmidt, D. A. Boardman, T. S. Steiner, M. K. Levings, A method for expansion and retroviral transduction of mouse regulatory T cells. *J. Immunol. Methods* **488**, 112931 (2021).

Acknowledgments: We thank L. Xu (BCCHR Flow Cytometry Core) for assistance in cell sorting, as well as T. Stach, Y. Chung, and B. Zhao (SBME-Seq) for assistance in performing and analyzing RNA-seq data. **Funding:** This work was supported by grants from Juvenile Diabetes Research Foundation (JDRF) Canada via the JDRF Centre of Excellence at UBC (grant key: 3-COE-2022-1103-M-B) and Canadian Institutes of Health Research (CIHR; FDN-154304). D.A.B. was supported by fellowships from CIHR and Michael Smith Health Research BC. S.M. was supported by a CIHR Graduate Scholarship (Master's Program; CGS-M), BCCHR CFKF Diabetes Research Studentships, and a UBC Four Year Doctoral Fellowship. M.K.L. is Canada Research Chair in Immune Engineering and receives a Scientist Salary Award from the BC Children's Hospital Research Institute. **Author contributions:** Conceptualization: D.A.B., J.K.G., A.J.L., and M.K.L. Methodology: D.A.B., S.M., J.K.G., M.M., T.H., Q.H., K.T., C.M.W., A.J.L., and M.K.L. Validation: D.A.B. and S.M. Formal analysis: D.A.B., S.M., and L.L. Investigation: D.A.B., S.M., J.K.G., L.L., V.C.W.F., M.H., M.M., T.H., Q.H., C.M.W., and A.B. Data curation: D.A.B., S.M., and L.L. Writing (original draft): D.A.B. Writing (review and editing): D.A.B., S.M. and M.K.L. Visualization: D.A.B. Supervision: D.A.B., S.M., and M.K.L. Project administration: D.A.B., S.M., M.M., and M.K.L. Funding acquisition: M.K.L. **Competing interests:** M.K.L. is an author on filed patents related to A2-CARs (PCT/CA2028/051167 and PCT/CA2018/051174, filed by the University of British Columbia UBC, published 28 March 2019). During the peer-review process, D.A.B. became an employee of AstraZeneca PLC and holds shares of AZN stock. The other authors declare that they have no competing interests. **Data and materials availability:** All data needed to evaluate the conclusions in the paper are present in the paper and/or the Supplementary Materials. RNA-seq data are deposited in NCBI's Gene Expression Omnibus and is accessible through GEO Series accession number GSE287328 (www.ncbi.nlm.nih.gov/geo/query/acc.cgi?acc=GSE287328); the code used for analysis is available on GitHub (https://doi.org/10.5281/zenodo.14674837).

Submitted 27 March 2025
Accepted 8 May 2025
Published 13 June 2025
10.1126/sciadv.adx7845